DEPARTMENT OF INTERNATIONAL AND EUROPEAN ECONOMIC STUDIES

ATHENS UNIVERSITY OF ECONOMICS AND BUSINESS

Land-use, climate change and the emergence of infectious diseases: A synthesis

William Brock

Anastasios Xepapadeas

Working Paper Series

24-09

March 2024

Land-use, climate change and the emergence of infectious diseases: A synthesis

March 29, 2024

William Brock[1] and Anastasios Xepapadeas[2]
[1]University of Wisconsin at Madison and University of Missouri at Columbia. E-mail: wbrock@ssc.wisc.edu

[2]Corresponding author: Department of Economics University of Bologna, and Athens University of Economics and Business,
E-mail: anastasio.xepapadeas@unibo.it

Land-use, climate change and the emergence of infectious diseases: An integrated model

Abstract

Scientific evidence suggests that anthropogenic impacts on the environment, such as land-use changes and climate change, promote the emergence of infectious diseases (IDs) in humans. We provide a synthesis which captures interactions between the economy and the natural world and links climate, land-use and IDs. We develop a two-region integrated epidemic-economic model which unifies short-run disease containment policies with long-run policies which could control the drivers and the severity of IDs. We structure our paper by linking susceptible-infected-susceptible and susceptible-infected-recovered models with an economic model which includes land-use choices for agriculture, climate change and accumulation of knowledge that supports land-augmenting technical change. The ID contact number depends on short-run policies (e.g., lockdowns, vaccination), and long-run policies affecting land-use, the natural world and climate change. Climate change and land-use change have an additional cost in terms of IDs since they might increase the contact number in the long-run. We derive optimal short-run containment controls for a Nash equilibrium between regions, and long-run controls for climate policy, land-use, and knowledge at an open loop Nash equilibrium and the social optimum and unify the short- and long-run controls. We explore the impact of ambiguity aversion and model misspecification in the unified model and provide simulations which support the theoretical model.

JEL Classification: I18, Q54, D81

Keywords: infectious diseases, SIS and SIR models, natural world, climate change, land-use, containment, Nash equilibrium, OLNE, social optimum, land-augmenting technical change

1 Introduction

The global carbon budget hourglass[1] predicted that if current emission levels – which for 2023 are estimated to be around 37.5GtCO_2 – persists there is a 50% chance that the global warming of 1.5°C relative to the preindustrial period could be exceeded in seven years. This maintains climate change and associated policies at the forefront of both the scientific and the policy agenda. Emissions from land-use change averaged at 4.7 GtCO_2per year for

[1]See https://globalcarbonbudget.org and Friedlingstein et al. (2023)

2013-2022 with a downwards trend (Friedlingstein et al. 2023) suggesting that emissions from land-use changes do not seem to be a big contributor to global emissions. Changes in land-use, however, apart from contributing to climate change have important impacts on the supply of ecosystem services. Winkler et al. (2021) estimated that between 1960 and 2019 land-use changes affected around 32% of global land area, with afforestation and crop abandonment in the global North, and deforestation and agricultural expansion in the global South. Gomez et al. (2021) review a large number of studies exploring the vulnerability of ecosystem services to land-use and land cover changes which are triggered by anthropogenic impacts, mainly socioeconomic, political and environmental factors, and feedbacks related to climate change. Land-use and land cover changes imply, therefore, potential vulnerability of provisioning, regulating, supporting and cultural ecosystem services.

The COVID-19 crisis, which emerged as both a serious human health emergency and a severe economic and social threat, brought to the forefront the link between the anthropogenic impact on the natural world, in the context of ecosystem services, and the emergence of infectious diseases (IDs). This link has been recognized in the literature related to IDs but not as much in the economic literature prior to the advent of COVID-19, although in the convergence model (Institute of Medicine, 2008), is indicated that social, political and economic factors, along with environmental and genetic ones, are leading factors in the emergence of IDs.

There is a considerable literature exploring the mechanisms underlying the emergence of IDs and seeking a basis for the design of efficient prevention policy, in which the anthropogenic impact has been identified as an important factor by a number of researchers. Scientific evidence suggests that the total number and diversity of outbreaks and richness of IDs have increased significantly since 1980 (e.g., Smith et al., 2014). ENSIA (2020), in a recent report, attributes the emergence of IDs such as COVID-19 to the destruction of habitats and loss of biodiversity, while Evans et al. (2020) point out that ecological degradation increases the overall risk of zoonotic disease outbreaks originating from wildlife. Watts et al. (2021), in the 2020 report of the Lancet countdown on health and climate change, emphasize that changing climatic conditions are increasingly suitable for the transmission of numerous IDs, while the recent statement of the Lancet COVID-19

Commission (Lancet, 2021, p. 21) indicates that "...most known emerging diseases have originated in non-human animals, usually wildlife, and have emerged due to environmental and socioeconomic changes, such as land-use change, agricultural expansion, and the wildlife trade."

Moreover, a recent report on COVID-19 (The Independent Panel for Pandemic Preparedness and Response, 2021) stresses that most of the new pathogens are zoonotic in origin and that land-use and food production practices and population pressure are driving their increasing emergence. They find that increasing tropical deforestation and incursion destroys wildlife health and habitat, and speeds interchange between humans, wildlife and domestic animals. They state that "The threats to human, animal and environmental health are inextricably linked, and instruments to address them need to include climate change agreements and "30x30" global biodiversity targets" (p. 19). Marani et al. (2021), using recent estimates of the rate of increase in disease emergence from zoonotic reservoirs associated with environmental change, suggest that the yearly probability of occurrence of extreme epidemics may increase due to deterioration of the natural world.

Confined animal feeding operations (CAFOs) have also been identified as a potential source of emerging IDs. The concern about CAFOs is that they harbor and provide a rich environment for the evolution of new strains of diseases. Furthermore, the use of antibiotics in CAFOs can also contribute to the emergence of antibiotic-resistant bacteria and may turn an emerging ID into an even more dangerous threat to human beings.[2] CAFOs require a large amount of land for the production of animal feed and the disposal of manure. Thus, the expansion of CAFOs has led to changes in land-use patterns, including the conversion of land to monoculture crops, and the disposal of manure on nearby fields.

In associating anthropogenic activities with the emergence of IDs, climate change is also significant. Scientific evidence (e.g., Wyns, 2020) suggests that infections which are transmitted through water or food, or by vectors such as mosquitoes and ticks, are highly sensitive to weather and climate conditions. The warmer, wetter and more variable conditions resulting from climate change are thus making it easier to transmit diseases such as malaria, dengue fever, chikungunya, yellow fever, Zika virus, West

[2]See, for example, Graham et al. (2008), Hollenbeck (2015), He et al. (2020), Guo et al. (2022) .

Nile virus and Lyme disease in many parts of the world. Furthermore, permafrost thaw, caused by climate change, also carries consequences in terms of increased risks of ID outbreaks as a result of live pathogens liberated from thawed permafrost (Walsh et al., 2018; Meredith et al., 2019).

Nova et al. (2022, Section 5) point out that the activities "that lead to anthropogenic disturbances of the environment – primarily, climate change, land-use change, urbanization, and global movement of humans, other organisms, and goods – affect societies and ecosystems in ways that favor the emergence of novel infectious diseases in human populations, expansions or shifts of diseases to new geographic regions, or re-emergence of diseases in various places." They provide links between disease transmission and changes in temperature and rainfall as well as between changes in land-use and disease incidence. For example, intensification of agriculture and industrial agriculture promotes *Aedes*-born viruses (e.g., dengue, Zika and yellow fever), Lyme disease and the Hendra virus. Mora et al. (2022) provide evidence of a large number of pathogenic diseases and transmission pathways aggravated by climatic hazards, thus revealing the magnitude of the human health threat posed by climate change and the urgent need for aggressive actions to mitigate greenhouse gas (GHG) emissions.

The discussion regarding the emergence of IDs suggests that the disease reservoirs, or ID hot spots, are located mainly in the tropical-subtropical climate zones in the Koepen-Geiger classification system (with the notable exception of permafrost). These climate zones contain hot spots for the natural world in terms of natural habitats, tropical forests and biodiversity. A disease outbreak which might emerge from the anthropogenic pressure and the impact of climate change on the disease reservoirs existing in hot spots, if it occurs, diffuses to the rest of the world through regular transportation channels. [3]

A possible path in analyzing the emergence, containment and prevention of ID could be a two-time-horizon set up. In the short run, in which the ID has emerged, public health control policies can be applied including vacci-

[3]ID hot spots may also exist in the temperate zone as development of CAFOs implies land-use changes. For example, the large amount of land needed for manure disposal may pollute water supplies thus making people more vulnerable to diseases. The concentration of animals makes CAFOs hot beds of disease, and increased use of antibiotics in CAFOs may lead to weakened effectiveness of antibiotics for humans. A list of health issues raised by CAFOs can be found at https://www.cdc.gov/nceh/ehs/docs/understanding_cafos_nalboh.pdf.

nations or containment policies such as lockdowns. In the long run, policies could focus on anthropogenic factors that affect the emergence and severity of IDs, such as climate change and changes in land-use. Thus, given the short-run, long-run aspects of IDs, their efficient management in both time horizons, requires coupled models of the economy and the natural world that captures this time separation. This approach parallels the development of integrated assessment models which couple the economy and climate, with an added time-separation component.[4]

The purpose of the present paper is to develop such a model and in particular a synthesis which captures interactions between the economy and the natural world and links climate, land-use and IDs. This is an extremely complex issue with many challenges as indicated clearly by Dangerfield et al. (2022).[5]In this synthesis we attempt to capture some aspects of this complex issue. In developing our model we use some elements from Brock and Xepapadeas (2020a) and Barbier (2021) in the coupling of SIR epidemics with land-use and climate change in a dynamic optimization framework. However, we move beyond these models, and our contribution relative to existing literature consists in the development of an integrated model, of the economy, land-use, climate change and infectious diseases using sub-models which are based on existing literature. Our synthesis incorporates disease dynamics; strategic behavior in static and dynamic frameworks; fast-slow dynamics or short-run, long-run analysis and their synthesis; land-use change and land-augmenting technical change as drivers of change in the natural world; energy use as a driver of climate change; spatial separation between North and South, and deep uncertainty and ambiguity aversion on

[4]There is an increasing body of literature that develops models that couple infectious diseases with the economy which focus on important aspects of the problem. or example the impact of pandemics in the context of multiple disasters (Martin and Pindyck, 2015); biodiversity loss and increased likelihood of zoonotic IDs (Augeraud-Véron et al., 2021); spillovers from animal hosts and CAFOs to humans in the context of changing land-use and climate change (Lo Iacono et al., 2016; Roberts et al., 2021); wildlife-human interactions in lower-middle income countries (Albers et al., 2020); the impact of land-use change on emerging IDs (Barbier, 2021); a general equilibrium "epi-econ" model that compares competitive equilibrium with welfare optimum (Boppart et al., 2020). The economic aspect of the COVID pandemic has mainly been studied in terms of ways to control the pandemic – lockdowns, social distancing, testing and isolation, reducing the speed of propagation, vaccine development, behavioral approaches – and the associated benefits and costs of these policies (e.g., Eichenbaum et al., 2020; Gollier, 2020; Thunström et al., 2020; Berger et al., 2021; Ashworth et al., 2022; Dobson et al., 2023)

[5]See also, Philipson (2000), Bloom et al. (2022)

policy instruments and their impact on policy design. Finally, we compare the welfare optimum with Nash equilibrium solutions in the long run in order to determine policies that can implement this optimum.

Our theoretical results, which are supported by numerical simulations, provide insights regarding: (i) containment policy design both between different models of ID spread and under ambiguity aversion regarding policy effectiveness in the short run, and (ii) land-use and climate policy to control the severity of the emerging IDs through their contact number in the long run, as well as suggestions about adjustments in valuation approaches for ecosystems and the calculation of the social cost of carbon when the emergence of IDs is taken into account. This approach has similarities to the Pike et al. (2014) approach of global strategies to thwart pandemics which consider adaptive strategies aiming at reducing the impact after a disease emerges – our short-run policy – or mitigation aiming at reducing the causes of pandemics – our long-run policy.

To capture spatial separation we develop a two-region model in which the tropical-subtropical zones are identified as region 1 and the temperate-snow zones as region 2. Sachs (2001) points out that agricultural technologies and health conditions are weak in the tropical relative to temperate zone, inducing a development gap. Therefore, a distinction between the two regions is relevant when land-use and disease impacts are concerned.

To capture time separation we consider two-stages with fast-slow dynamics. In the first stage, which we call the short-run, the outbreak of the ID has occurred. After the outbreak, both regions introduce policies to contain/eliminate the epidemic. Throughout the paper we assume that containment policies in the short run are decided in each region in a non-cooperative way. This assumption draws on the fact that national health policies during the COVID-19 period have been decided by an independent national health system based on the specific characteristics of each country and not by a supranational authority.[6] In designing containment policies in the short run, the regions do not consider any anthropogenic impacts on the specific characteristics of the ongoing ID.

In the second stage, which we call the long-run, the regions take into

[6]Note that in the implementation of the Paris Accord, countries commit to carbon emissions paths. It is reasonable to assume that these paths are decided with reference to own welfare. This leaves open the possibility of strategic interactions.

account the evolution of climate change and the encroachment on the natural world by agricultural activities, on the emergence of the ID. The long-run policies relate, therefore, to the regulation of land-use which-directly affects disease characteristics, as well as to the adequate control of temperature increase relative to the preindustrial period through climate policy. We think that the fast-slow dynamics framework is reasonable because the type of policies appropriate for containment once the diseases emerges, and the type of policies appropriate for long-run prevention are very different and operate at different time scales. The fast-slow approach can, therefore, provide a clear picture of the distinct policies required.

2 Natural world and climate change.

Let $R(t)$ represent the natural world which provides ecosystem services but also includes the viral-host reservoir for IDs. Human encroachment and destruction of the natural world emerges through changes in land-use due mainly to land-intensive agriculture.[7] This introduces a tradeoff between output production, ID emergence and its severity which can expressed terms of the basic reproduction number.[8] Land-intensive industrial agriculture will reduce the natural world and potentially facilitate the emergence of IDs. Let the natural world R_i in each region $i = 1, 2$ be defined as:

$$R_i(t) = \bar{L}_i(t) - L_{A,i}(t) \ , R_i(t) \geq 0, \tag{1}$$

where $\bar{L}_i(t)$ represents aggregate land availability, and $L_{A,i}(t)$ land devoted to agriculture in each region respectively. Reduction of R_i, as agricultural activities expand, indicates a reduction in the "distance" between human activities and disease reservoirs.[9]

In considering the impact of climate change, we assume that energy production by fossil fuels generates emissions of GHGs. Let $X(t)$ denote the stock of GHGs at time t relative to the preindustrial period with temporal evolution according to:

$$\dot{X}(t) = E_1(t) + E_2(t) - dX(t) \ , X(0) = X_{preindustrial}, \tag{2}$$

[7] We do not consider urbanization as a source of encroaching on the natural world.

[8] The basic reproduction number denoted by R_0 , is defined as the average number of secondary infections produced when one infected individual is introduced into a host population where everyone is susceptible.

[9] Restoration activities, such as reforestation, REDD+ policies and payments for ecosystem services, could increase R_i. To simplify the model, we do not include such activities.

where $E_i(t)$ denotes emissions of GHGs from each region and d is a small GHG depreciation parameter. The accumulation of GHGs increases global average temperature relative to the preindustrial level (the temperature anomaly).[10] Using Matthews et al.'s (2009) approximation with Λ_i representing the regional transient climate response to cumulative carbon emissions (RTCRE)(see Leduc et al., 2016), the temperature anomaly relative to the preindustrial temperature levels can be defined, in each region, as:

$$T_i(t) = \Lambda_i X(t) \ , T_i(0) = 0. \tag{3}$$

Climate change is induced by positive temperature anomaly that generates damages to the economy.

3 The epidemiological models

Hethcote (2000, Figure 1) describes a general epidemiological model with an MSEIR transfer diagram that links flows between the passively immune class M, the susceptible class S, the exposed class E, the infective class I, and the recovered class R, with the passively immune class M and the latent period class E often being omitted because they are not crucial for the susceptible-infective interaction. If recovery does not provide immunity, then the model is called an SIS model, since individuals move from the susceptible class to the infective class and then back to the susceptible class upon recovery, while if individuals recover with permanent immunity, then the model is an SIR model. As Hethcote (1988, p. 123) points out, SIR models are appropriate for viral agent diseases such as measles, mumps, and smallpox, while SIS models are appropriate for some bacterial agent diseases such as meningitis, plague, and venereal diseases, and for protozoan agent diseases such as malaria and sleeping sickness. The common cold is also an SIS disease since infection does not confer any long-lasting immunity.

To introduce the integrated model we follow Hethcote (1988, 2000) and consider a simple two-region mathematical model for an ID which could be SIR or SIS, with regions indexed by $i = 1, 2$ for the tropical and temperate zones respectively with susceptibles denoted by S_i, infectives by I_i, and

[10] The accumulation Eq. (2) can be augmented by allowing for an increase in the natural world to slow down GHGs accumulation in its capacity as a carbon sink. In this case agricultural expansion would further increase GHGs accumulation and induce another positive feedback on the ID's contact number. This feedback could be an interesting area for further research.

recovered by R_{ei}.

3.1 The SIR model

The simple SIR model in terms of fractions of the total population can be written, in continuous time, as[11]:

$$\dot{S}_i(t) = -\lambda_i(t) I_i(t) S_i(t), \; S_i(0) > 0 \tag{4}$$

$$\dot{I}_i(t) = \lambda_i(t) I_i(t) S_i(t) - \gamma_i I_i(t) \;, \; I_i(0) > 0 \tag{5}$$

$$R_{ei}(t) = 1 - S(t) - I(t) \;, \; i = 1, 2, \tag{6}$$

where $\lambda_i(t)$ is the regional contact rate, γ_i is the recovery or removal rate, and $\sigma_i(t) = \lambda_i(t)/\gamma_i$ is the regional contact number.[12] We will deviate from Hethcote here by assuming that λ_i is not a positive constant, but it may change along a policy path. From Hethcote (1989, Theorem 5.1), we have that if $\sigma_i \leq 1$, then $I_i(t)$ decreases to zero as $t \to \infty$. If $\sigma_i > 1$, then $I_i(t)$ first increases to I_i^{max} and then decreases to zero with

$$I_i^{max} = 1 - \frac{1}{\sigma_i} - \frac{\ln \sigma_i}{\sigma_i}, \tag{7}$$

In the SIR model, since $I_i^{\infty} = 0$, at a steady state $S_i^{\infty} + R_{ei}^{\infty} = 1$.

3.2 The SIS model

The simple SIS model in terms of fractions of the total population can be written, in continuous time, as:

$$\dot{S}_i(t) = -\lambda_i(t) I_i(t) S_i(t) + \gamma_i I(t) \;, \; S(0) > 0 \tag{8}$$

$$\dot{I}_i(t) = \lambda_i(t) I_i(t) S_i(t) - \gamma_i I_i(t) \;, \; I_i(0) > 0 \tag{9}$$

$$I_i(t) + S_i(t) = 1 \;, \; i = 1, 2. \tag{10}$$

From (10), the dynamic system can be written as:

$$\dot{I}_i(t) \;\; = \;\; \gamma_i I(t) \left[\sigma_i(t) \left(1 - I_i(t)\right) - 1\right]. \tag{11}$$

From Hethcote (1989, Theorem 4.1) we know that the solution for $S_i(t)$ approaches $1/\sigma_i(t)$ as $t \to \infty$ if $\sigma_i > 1$, while it approaches 1 as $t \to \infty$ if $\sigma_i \leq 1$. This implies that the SIS dynamics relax to the steady state

[11] To simplify the exposition we do not consider vital dynamics (births or deaths). Vital dynamics can be introduced by allowing an inflow of newborns and an outflow of deaths. If deaths balance births the population will remain constant (Hethcote 2000). In this case the qualitative properties of our results will not change.

[12] We define R_0, the basic reproduction number, as $R_{0i} = \sigma_i$. For details regarding R_0, see Delamater et al. (2019).

$S_i = \min\{1, 1/\sigma_i\}$ and $I_i = 1 - S_i$ for any point in time.

Thus in both SIR and SIS models the contact number $\sigma_i(t)$ is the threshold quantity with the critical threshold value 1. We consider a time-dependent contact number $\sigma_i(t)$ since it could refer to different emerging IDs at different points in time, or change over time in response to policies.

4 The integrated model.

In this section we link, natural world, climate change, epidemics and the economy in order to develop an integrated model.

4.1 Infectious diseases natural world and climate change

Let an SIR-type epidemic emerge in the interval $[t_0, t_0 + dt]$. It is reasonable to assume that the major impact of the epidemic will be realized in the neighborhood of I_i^{max} defined by (7). The sensitivity of I_i^{max} to the contact number σ_i is given by the derivative $\frac{dI_i^{max}}{d\sigma_i} = \frac{\ln \sigma_i}{\sigma_i^2} > 0$ for $\sigma_i > 1$. Thus potential reduction of the contact number by public health containment policy or long-run land-use/climate change policies are expected to reduce the major impact of the epidemic. At the maximum share of infectives, the share of susceptibles and recovered will be

$$S_i + R_{ei} = 1 - I_i^{max} = \frac{1}{\sigma_i} + \frac{\ln \sigma_i}{\sigma_i} = x_i(1 - \ln x_i) = f_i(x_i)\,,\ x_i = \frac{1}{\sigma_i}. \quad (12)$$

In order to incorporate the economic forces affecting the contact number into the SIR model, we write for $i, j = 1, 2,\ i \neq j$:

$$x_i = \min\{1, 1/\sigma_i\} \quad (13)$$

$$\frac{1}{\sigma_i} = \phi_{0i}(R_1, T_1) + \phi_{1i}\left[b_i v_i - q_j\left(1 - S_j - R_{ej}\right)\right]. \quad (14)$$

In (14) ϕ_{0i} is the part of the contact number which is exogenous relative to short-run containment policies and depends on the state of the natural world (i.e. land-use and temperature). We will call this part the "natural" contact rate which in our model can be affected by long-run policies. Since region 1 – the tropical/subtropical region – is regarded as containing the disease reservoirs (that is, the hot spot for the emergence of IDs), it is assumed that the value of ϕ_{0i} is determined by the current state of the natural world, $R_1(t)$, along with the current temperature anomaly, $T_1(t)$,

in the region. In the long run, encroachment of the natural environment due to changes in land-use and agricultural expansion – which "reduces" the natural world – along with global warming increase the contact number. We assume, therefore, that

$$\phi_{0i}\left(R_1, T_1\right) = \phi_{0iR}(R_1(t)) + \phi_{0iT}(T_1(t)) \geq 0, \tag{15}$$

where $\phi_{0iR}(R_1(t)), \phi_{0iT}(T_1(t))$ are concave increasing, convex decreasing respectively.[13]

The $\phi_{0i}\left(R_1(t), T_1(t)\right)$ function is decreasing in R_1 since it is assumed that augmenting the natural world in the South (i.e., reducing the relative size of the disease reservoirs and increasing their distance from human activities) reduces the contact number in both regions for any specific epidemic. On the other hand, global warming in the South increases the contact number for both regions, thus the function is increasing in T_1.

The term ϕ_{1i} characterizes the effectiveness of the containment policy in each region. In the short run, containment effort $v_i\left(t\right)$ reduces the contact number $\sigma_i\left(t\right)$, with effectiveness b_i and convex costs $c_i\left(v_i\left(t\right)\right)$. For an SIR epidemic, v_i could be interpreted as vaccination.[14] We assume no migration between regions,[15] but individuals from one region can make short visits to the other by regular means of transportation (e.g., airplanes, ships). Infected individuals from region j traveling to region i infect individuals in region i proportionally to those infected in region j and vice versa, with proportionalities (q_j, q_i) respectively.

To incorporate economic forces into the contact rate of an SIS-type epidemic, assume that the SIS model evolves in fast time. This implies:

$$\epsilon \dot{S}_i\left(t\right) = \left(1 - S_i\left(t\right)\right)\left[\lambda_i(t) S_i(t) - \gamma_i\right].$$

[13]Since IDs seem to be always emerging, throughout this paper we make the plausible assumption that in the short-run equilibrium and the long-run optimum, $0 < \phi_{0i}\left(R_1(t), T_1(t)\right) < 1$. For the linear specification (15) this requires a certain parametrization which we use in the simulation part. Alternatively the specification $\phi_{0i}\left(R_1(t), T_1(t)\right) = \left(1 - \mathrm{e}^{-\alpha_1 R_1}\right)\left(\mathrm{e}^{-\beta_i T_1}\right)$ for positive α_i, β_i could have been used. We did not use this specification to simplify the calculations.

[14]We do not consider waning immunity issues related to vaccination.

[15]Considering the possibility of IDs from large-scale migration flows between the two regions is beyond the scope of this paper, but it is an interesting area for further research.

For $\epsilon \to 0$ the fraction of susceptibles is determined as:

$$S_i(t) = \min\{1, 1/\sigma_i(t)\}, \frac{1}{\sigma_i(t)} = \tag{16}$$
$$\phi_{0i}(R_1(t), T_1(t)) + \phi_{1i}[b_i v(t) - m_i^{as} S_i(t) - q_j(1 - S_{jt})]$$

$$I_i(t) = 1 - \frac{1}{\sigma_i(t)}, \; i, j = 1, 2, \; i \neq j. \tag{17}$$

The contact number defined in (16) has a similar interpretation to the SIR case. If vaccination is not a relevant public health policy for an SIS epidemic, then v_i can be interpreted as an intervention to lower σ_i, perhaps masking or isolating the patient from healthy individuals, etc. The contact number increases, in the SIS case, by the potential spread of the disease by asymptomatic infecteds at the rate $m_i^{as} \geq 0$.

To simplify the mathematical exposition, when we write the optimality conditions we assume solutions in the zone $\sigma_i \geq 1$, or equivalently $S_i \leq 1$ for both types of epidemics.[16]

[17]

4.2 The economy

To embody the economy into the framework defined above, we introduce a composite good:

$$Z_i(t) = C_i(t)^{\hat{a}_i} R_i(t)^{\hat{b}_i}, \hat{a}_i > 0, \hat{b}_i > 0, \hat{a}_i + \hat{b}_i < 1, i = 1, 2, \tag{18}$$

[16] Although the relevant part of the contact rate in both regions depends on (R_1, T_1), the value of the contact rate need not be the same since it might depend on regional characteristics. That is, in general we may expect $\phi_{01}(\cdot,\cdot) \neq \phi_{02}(\cdot,\cdot)$. At this stage we were not able to provide a quantitative indication of this distinction. In Section 6 we make this distinction arbitrary since our objective is to validate the theoretical model. Undoubtedly issues related to the exact source of IDs and the regional impacts of encroachments, CAFOs, and increasing temperatures on the strength of emerging IDs is an important area of future interdisciplinary research which could improve epi-econ models.

[17] It should be noted, however, that although in this paper we treat the tropics as the main source of emerging IDs, the CAFOs of industrial agriculture in the temperate zones are also breeding grounds for IDs. If the expansion rate of IDs from CAFOs proceeded at a rate comparable to the expansion rate of IDs from encroachment into the tropics (e.g., the deforestation rate of the Amazon for soybeans and cattle), then $R_2(t)$ – and potentially $T_2(t)$ – should affect ϕ_{0i}. Furthermore, Mora et al. (2022) list 1,006 different pathways for IDs and around half of them are aggravated by climate change. Increasing temperatures might increase IDs coming out of temperate zone CAFOs, with animals being weakened by crowding and temperature stress, along with an increase in IDs coming out of the tropics. To keep the theoretical model as tractable as possible, we do not take into account the impact of temperate zones and consider only the tropics as a source of IDs.

where C denotes material inputs in the composite good and R is Nature's input into the composite good (that is, ecosystem and biodiversity services). We define utility in each region as:[18]

$$U_i\left(Z_i(t)\right) = \ln\left(C_i(t)^{\hat{a}_i} R_i(t)^{\hat{b}_i}\right). \tag{19}$$

Material inputs are produced by labor, energy and land devoted to land-intensive industrial agriculture.[19] Labor is offered by susceptibles – who are not contained by lockdowns – and is allocated among the non-agricultural part of the material inputs, $l_{c,i}$, and the land-intensive agriculture, $l_{A,i}$. Land devoted to agriculture can be augmented by innovation in agricultural technologies such as biotechnology. The accumulated stock of knowledge, denoted by N, acts as Harrod augmenting technical change in the agricultural sector with innovation augmented land, or effective land input, defined as $(NL_{A,i})$.[20] Knowledge accumulates according to:

$$\dot{N}\left(t\right) = n_2\left(t\right) - mN\left(t\right),\ N\left(0\right) = 1, \tag{20}$$

where $n_2\left(t\right)$ is the innovation flow undertaken by the developed North region 2 (e.g., R&D in bioengineering). The initial condition corresponds to the no innovation case, and m is a rate at which accumulated knowledge becomes obsolete. In defining knowledge dynamics by (20), we follow (Hall et al., 2010, Eq. 18), with a change to continuous time. In this specification the stock of knowledge is constructed from a string of R&D investment and depreciates at a certain rate, with depreciation indicating the rate of exit of R&D expenditure from the stock of knowledge.[21] Innovation is costly and innovation costs c_{ni} fractionally lower the composite good. It is assumed that knowledge has public good characteristics and, once accumulated in the North, is freely available to both regions.[22]

[18]The log-linear utility function defined here can be regarded as a special case of a more general CES utility function of the form $Z = [aC^{\tau} + (1-a)R^{\tau}]^{1/\tau}$with elasticity of substitution between material inputs and Nature $\sigma_e = 1/(1-\tau)$. This more general formulation might be used to explore the impact of complementarities between material inputs and Nature as measured by the inverse of the elasticity of substitution for $\sigma_e < 1$.

[19]To simplify the model, we do not include capital formation.

[20]Barrows et al. (2014) point out that genetically engineering seed adoption can produce non-trivial savings of land from conversion to traditional agriculture as well as of emissions of GHGs. Agricultural productivity could also be improved by automation and robotics (e.g., Biswas and Aslekar, 2022).

[21]We realize that this specification may be "too simple" a representation of the dynamics of knowledge accumulation but going to a more complicated specification adds yet another level of complexity to an already complex dynamical system.

[22]An alternative assumption could be that knowledge is accumulated in both regions

Furthermore, costs related to labor use, $w_{l,h,i}$; land-use, $c_{L,i}$; energy, $c_{h,E,i}$; containment of the epidemic, $c_{v,i}$; climate damages, ω_i; and R&D innovation in agriculture, $c_{n,2}$, fractionally lower the material part of the composite good.[23] After dropping t to ease notation, the composite good can be defined, for $i = 1, 2$, as:

$$C_i = \left[\left(l_{c,i}^{\beta_{l,c,i}} E_{c,i}^{\beta_{c,E,i}}\right)^{\alpha_{c,i}}\right] \times \left[\left(l_{A,i}^{\beta_{l,A,i}} \left(NL_{A,i}\right)^{\beta_{L,A,i}} E_{A,i}^{\beta_{E,A,i}}\right)^{\alpha_{A,i}}\right] \times$$
$$\exp\left[-\left(\sum_h w_{l,h,i} l_{h,i} + c_{L,i} L_{A,i} + \sum c_{E,h,i} E_{h,i} + \right.\right. \tag{21}$$
$$\left.\left.\frac{c_{v,i} v_i^2}{2} + \frac{\omega_i T_i^2}{2} + \frac{c_{n,i} n_2^2}{2}\right]\right.$$

$$h = c, A,\ c_{n,1} = 0, c_{n,2} > 0 \tag{22}$$

$$S_i = l_{c,i} + l_{A,i} \tag{23}$$

$$R_i = \bar{L}_i - L_{A,i}. \tag{24}$$

Regional utility defined on the basis of (21) could include more types of disease related costs, apart from the impact on labor force, such as for example the disease burden. This could be added in (21) as another factor lowering the composite good such as, $\left[c_{D,i}(1 - S_i)^2\right]/2$. Adding more disease cost components is left to future research.

We study the optimal management of the integrated model in the context of two different time frames. In the first – the short-term management – the epidemic has emerged and the objective is to choose containment control, labor allocation and energy use to maximize utility. In this short time horizon, the regional natural world, temperature anomaly, and knowledge (R_i, T_i, N) are considered as fixed, since their evolution is slow relative to the the evolution of the pandemic and the primary objective is the containment of the pandemic. In this time frame, the short-term optimal controls depend parametrically on (R_i, T_i, N).

since many research labs in agriculture also do R&D for agricultural efficiency in tropical zones. Then $n_2(t)$ in (20) should be replaced by $(n_1(t) + n_2(t))$. Another assumption could be that knowledge is a private good to each sector with partial diffusion across regions. If knowledge is undertaken in both regions then strategic aspects could be included in the process where regions choose their optimal inputs to knowledge accumulation (e.g. Xepapadeas, 1995).

[23] REDD+ activities can be introduced by adding a term $RD0$ for REDD+ to the right hand side of (24) and including a cost for these activities which fractionally reduces the composite good.

In the second – the long-term management – it is assumed that the emerged ID, which is the fast system, has been optimized and relaxed to a steady state which depends parametrically on the natural world R_1 and the evolution of regional temperature T_1 which is slow relative to the evolution of the ID. As (R_1, T_1, N) evolve, the short-run optimal controls for the management of the epidemic system also evolve. The relation between the epidemic system and the natural world is reflected in (15), which is the policy-independent – in the short run – component of the contact number.

For reasons explained in the introduction, we focus in the short run on noncooperative solutions in which each region maximizes own welfare. For a social optimization management problem, a social planner would maximize the global welfare indicator which could be defined as:

$$W = \ln\left(Z_1^{z_1} Z_2^{z_2}\right). \tag{25}$$

This problem will be examined in the long term horizon.

4.3 Policy design

We assume that short-run containment and long-run prevention policies will target the contact number σ, directly for short-run containment and indirectly for long-run prevention which will include slow drivers such as land-use and climate change. The main impact on the economy from the ID will be loss of output because of a reduction in output-producing labor.[24] For both the SIR and the SIS models the maximum reduction in output-producing labor is $1-I_i$. After the emergence of the ID costly policies such as vaccination or lockdowns will reduce the contact number. The fraction of recovered or susceptible individuals should be increasing both in short-run containment policies once the disease emerges, but also in long-term prevention policies.

Once an ID has emerged, the time length of public health management after its emergence is not very long relative to the time scale of the evolution of land-use and climate change. For example the 1918 flu lasted 1-2 years, the major SARS outbreak lasted 8 months, the H1N1 lasted approximately

[24]The output-producing labor force in the SIS case could include workers who are asymptomatic in the sense that, although infected, they do not have symptoms that require treatment, so they are neither in the infected class nor in quarantine but can spread the disease and increase the contact number.

two years, while the major impact of the COVID-19 pandemic lasted 3-4 years (although it is still ongoing). Thus our modeling introduces a sequence of epidemics, each of which could have a specific contact number.

The time sequence of events and policies which are considered in our model shown in Fig. 1 can be described as follows: (1) Design optimal policy for land-use change/CAFOs/climate change; (2) An ID emerges: apply public health control during duration of that EID; (3) After containment of the ID, keep designing optimal land-use change/CAFOs/climate change;[25] (4) Another ID emerges: apply public health control; (5) After containment of this ID, keep designing optimal policy for land-use change/CAFOs/climate change, and so on. In our model the public health control period is the short-run or containment period.

{Insert Figure 1 here}

We use continuous time and think of the "instant" in which an ID emerges as a "short period" like 1-2 years. When the ID arrives the contact number is fixed but it can be lowered by public health policies Then the long run optimization can be interpreted as as optimization over an infinite number of consecutive "short periods" in which realistically we will experience a sequence of emerging IDs. In the long run there are incentives to adopt land-use change/CAFOs/climate change policy so that the contact number of the ID emerging at the "next instant" is lower.[26]

5 Short-run disease containment

We study the optimal containment problem in regions $i = 1, 2$ once the epidemic has emerged. In this case the planners take the natural world $R_1(t)$, the stock of knowledge $N(t)$, and the temperature anomaly $T_1(t)$ as exogenous, and decide about the public health policy $v_i(t)$, along with labor allocation and energy use. Thus the controls for the short-run problem are $u_i = (l_{c,i}, E_{c,i}, l_{A,i}, E_{A,i}, v_i)$. The solution concept for public health policy will be a noncooperative Nash equilibrium solution in which the region's

[25] We mention CAFO although we do not analyze CAFO policies to suggest extensions of policy regimes.

[26] If we used discrete time we would define S, I, R_e in each period $[t, t+1]$. The advantage of continuous time formulation is that the results are easier to interpret as well as being more elegant, without any significant qualitative difference relative to the discrete time formulation.

planner maximizes own regional welfare, taking the actions of the other region as given. Given that during the COVID-19 pandemic countries have mainly designed disease containment policies unilaterally though their own health systems, the Nash equilibrium concept might be a realistic representation.

5.1 Noncooperative solutions

We start with the SIS case which is relatively simpler.

5.1.1 SIS epidemics

In the SIS model labor supply is determined by the susceptibles, that is, $S_i = l_{c,i} + l_{A,i}$. Assuming that the objective is to contain and/or eliminate the epidemic, then the short-run time problem for the instant of the SIR, with fixed R_1,T_1 dropping t to ease notation, is:

$$\max_{u_i} \ln Z_i \ \text{, subject to} \tag{26}$$

$$S_i = l_{c,i} + l_{A,i} \tag{27}$$

$$\hat{S}_i = \bar{\varphi}_{0i} + \varphi_{1i}\left[b_i v_i - q_j\left(1 - S_j\right)\right] \tag{28}$$

$$S_i = \min\left\{\hat{S}_i, 1\right\} \tag{29}$$

$$\bar{\varphi}_{0i} = \frac{\bar{\phi}_{0i}}{1 + \varphi_{1i} m_i^{as}}, \varphi_{1i} = \frac{\phi_{1i}}{1 + \varphi_{1i} m_i^{as}}, \tag{30}$$

with $\bar{\varphi}_{0i}$ being the part of the contact number which is independent of short-term policies. As shown analytically in Appendix 1 the optimal containment policy is defined as:

$$v_i^* = \left(\frac{\varphi_{1i} b_i}{\hat{a}_i c_{v_i}}\right) \zeta_i(S_j),$$

where ζ_i is the Lagrangian multiplier associated with the constraints defined by combining (27)–(29), and the the best response functions are nonlinear of the form

$$S_i \ = \bar{\varphi}_{0i} + \varphi_{1i}\left[b_i\left(\frac{\varphi_{1i} b_i}{\hat{a}_i c_{v_i}}\right)\zeta_i(S_j) - q_j\left(1 - S_j\right)\right] \quad i, j = 1, 2, i \neq j. \tag{31}$$

At the Nash equilibrium solution the susceptibles (i.e., non-infecteds in each region) act as strategic complements, so the containment effect in one region will help the other region.[27] The result is shown more clearly in the

[27]For similar results in the literature of infection/invasion control see Fenichel et al.

simulations in Section 6. Once $\left(S_1^N, S_2^N\right)$ are obtained, then by substitution into (70) the Nash equilibrium values for the regional optimal containment policy are obtained.

Finally, we can explore the question of what the minimum size $\hat{R}_1$ is for the natural world so that a disease, if it emerges in a virus reservoir of region 1, will not spread because the contact number is below 1 (i.e., $\sigma_i(t) < 1$, $i = 1, 2$). In such a case, no containment is required and $v_{it}^* = 0$. Using (28) and setting $S_i(t) = S_j(t) = 1$, $\hat{R}_1$ can be defined for any given temperature anomaly as the minimum value of R_1 such that $(\bar{\varphi}_{0i}(R_1(t); T_1(t))) \geq 1$, since in this case $\bar{\varphi}_{0i}(R_1(t); T_1(t)) = 1/\sigma_i(t)$. We will call this value the ID safe threshold. If $R_1(t) < \hat{R}_1$ for some time t, an emerging ID will spread in at least one of the two regions and may invade the second region through transport. The containment of the disease in this case requires costly interventions.

5.1.2 SIR epidemics

To determine the impact of an SIR epidemic on labor supply, we need to note that at an SIR steady state the share of infectives tends to zero, which is not the case for an SIS epidemic. In this case we approximate the impact on labor supply by the maximum share of infectives, I_i^{max} in the emergence interval $[t_0, t_0 + dt]$, so that labor supply is given by $\mathcal{Z}_i = 1 - I_i^{max}$ (see 12).[28] Using (13) and (14) we obtain the share of non-infectives, $\mathcal{Z}_i$, which corresponds to the maximum number of infectives, that determines greatest impact on labor supply,

$$\mathcal{Z}_i = S_i + R_{ei} = 1 - I_i^{max} = \frac{1}{\sigma_i} + \frac{\ln \sigma_i}{\sigma_i} \tag{32}$$

$$l_{c,i} + l_{A,i} = \mathcal{Z}_i = \frac{1}{\sigma_i}\left[1 - \ln\left(\frac{1}{\sigma_i}\right)\right] = x_i(1 - \ln x_i) = f_i(x_i(v_i)) \tag{33}$$

$$x_i(v_i) = \frac{1}{\sigma_i} = \left[\bar{\phi}_{0i} + \phi_{1i}\left[b_i v_i - q_j(1 - \mathcal{Z}_j)\right]\right], \tag{34}$$

with $\bar{\phi}_{0i}$ being the part of the contact number which is independent of short-term policies. As shown in Appendix 2, the the optimal choice for v_i which is chosen to control I_i^{max} is implicitly defined as the solution of

$$F_i(v_i, \mathcal{Z}_j, \zeta_i) = -\hat{a}_i c_{vi} v_i - \zeta_i \phi_{1i} b_i \ln\left(\bar{\phi}_{0i} + \phi_{1i}\left[b_i v_i - q_j(1 - \mathcal{Z}_j)\right]\right) = 0. \tag{35}$$

(2014), Reeling et al. (2015), Bloom et al. (2022).

[28] For $R_0 = 0, S_0 = 1$, Fig. 8 of Hethcote (1989) implies $I^{max} = 0.34$, while Fig. 3 of Hethcote (2000) implies $I^{max} = 0.34$.

Since the optimal containment policy for the SIR epidemic is more complex than the SIS case, some insights into this policy can be obtained by assuming that $q_j = 0$ to simplify. Then if $\bar{\phi}_{0i} + \phi_{1i} b_i v_i^* = 1$ the optimal policy will be $v_i^* = 0$. In this case choosing a policy $\hat{v}_i$ such that

$$\bar{\phi}_{0i} + \phi_{1i} b_i \hat{v}_i = 1,$$

will be sufficient control to block that SIR epidemic. Assuming that the "natural" contact number is $0 < \bar{\phi}_{0i} < 1$ and considering that IDs seem to be always emerging, it seems plausible that the optimal short-run policy requires $v_i^* > 0$. A Nash equilibrium short-run containment policy can also be characterized as shown in Appendix 2.

5.1.3 SIS vs SIR containment policy

To provide a clear comparison between the optimal containment policies for SIR or SIS epidemics, we consider a subproblem stemming from (21) in which there is only one region and the composite consumption good is produced by labor only. In this case the problem is

$$\max_l \alpha \ln l - wl - \frac{cv^2}{2}, \text{ subject to}$$

$$l = S = \phi_0 + \phi_1 bv \text{ for SIS}$$

$$l = S + R_e = (\phi_0 + \phi_1 bv)\left[1 - \ln(\phi_0 + \phi_1 bv)\right] \text{ for SIR.}$$

Proposition 1. *Let v_{SIS}^* and v_{SIR}^* be the short-run optimal containment policies for the SIS and the SIR models respectively derived from the one region subproblem. Then $v_{SIR}^* < v_{SIS}^*$.*

For the proof see Appendix 3.

The proposition is illustrated in figure 2, where for the same marginal cost for the ID the marginal benefit curve for the SIR is below the corresponding curve for SIS.

{Insert Fig. 2 here}

A possible intuition behind this proposition could be that the presence of the recovered in an SIR epidemic requires less containment effort than an SIS epidemic that has no recovery and a share of infected remains at the steady state. The result can be changed if, in addition to the standard cost

of the epidemic in terms of labor supply, other costs such as loss of life which are different for SIR and SIS epidemics are included.

We conjecture that in the two-region model the assumption $\frac{1}{\sigma} < 1$ will remain plausible since adding the term $-q_j\left(1-\mathcal{S}_j\right)$ will tend to further reduce $\frac{1}{\sigma}$. Thus we expect that at the Nash equilibrium the results $v^*_{SIR} < v^*_{SIS}$ will hold. For the full model (21), however, comparisons require extensive numerical analysis which is beyond the objectives of the present paper.

6 Disease prevention in the long run: climate change, natural world preservation and innovation

In Section 5 we studied disease containment in the short run by assuming that the ID has already emerged. In the short run, the allocation of the regional land between agriculture and preservation, and the regional temperature anomalies were treated as exogenous parameters. In the long run, however, land-use can change, while temperature will evolve in response to the use of fossil fuels and climate policies. Changes in land-use which might reduce the natural world and bring human activities closer to disease reservoirs, along with an increase in regional average temperatures, will affect the long-run path of the natural contact rate ϕ_{0i}, which is basically independent of short-term containment policies. Treating dt as an "episode" which is managed optimally by public health policies provides insight into the containment problem. Then the long-run problem captures abstractly the problem of management of infinitely repeated episodes and indicates strong incentives for long-run land-use and climate management.

6.1 Noncooperative long-run prevention

To study noncooperative solutions in the long run, we assume that each region takes as given the initial temperature anomaly and the initial stock of knowledge and commits to the emission and innovation paths (region 2 only) that optimize own welfare functions, given the best response of the other region. The solution of this problem will characterize an open-loop Nash equilibrium (OLNE).[29] In the long-run analysis we consider the case of SIS

[29]The concept of the OLNE could be interpreted as a situation in which the regions decide to commit to a future path of land-use/climate policy at the beginning of an agreement. This type of equilibrium concept might not be as satisfactory – in terms of

epidemics only. The consumption flow for the long-run problem is obtained by substituting the fast-time (short-run) optimal controls for containment $v^*_{SIS,i}$ into $\hat{S}_i$ to obtain the short-run Nash equilibrium levels of susceptibles S^N_i. For a sequence of SIR epidemics the approach would be to define the maximum share of infectives which determines the maximum impact on labor supply during the episode by the optimized share of infectives as defined in Section 5.1.2 and use $v^*_{SIR,i}$ to define the consumption flow. The analysis is then the same as in the case of the SIS epidemic.

The control problem for region i in the time scale of the climate change can be written as:

$$J^N_i = \max_{\{u_i(t),R_i(t),n_i(t)\}} \int_0^\infty \mathrm{e}^{-\rho t}\left[\hat{a}_i \ln C_i(t) + \hat{b}_i \ln R_i(t)\right] dt, \tag{36}$$

subject to (1)-(3) and (27)-(30), with $\rho > 0$ the utility discount rate, and with controls and states respectively as

$$\mathbf{u}_i(t) = (l_{c,i}(t), l_{A,i}(t), L_{A,i}(t), E_{c,i}(t), E_{A,i}(t), n_2(t)), \ \mathbf{x} = (X, N).$$

In this optimization problem, after dropping t to ease notation, the following constraints apply:

$$\hat{S}_i = \varphi_{0i}(R_1, T_1) + \varphi_{1i}\left[b_i v^*_i\left(S^N_i\right) - q_j\left(1 - S^N_j(t)\right)\right] \tag{37}$$

$$S_i = \min\left\{\hat{S}_i, 1\right\} \tag{38}$$

$$\varphi_{0i}(R_1, T_1) = \frac{\phi_{it}(R_1, T_1)}{1 + \phi_{1i} m^{as}_i}, \varphi_{1i} = \frac{\phi_i}{1 + \varphi_{1i} m^{as}_i} \tag{39}$$

$$R_i = \bar{L}_i - L_{A,i} \tag{40}$$

$$S_i = l_{c,i} + l_{A,i} \tag{41}$$

$$E_i = E_{c,i} + E_{A,i} \tag{42}$$

$$T_i(t) = \Lambda_i X(t), \tag{43}$$

where $\varphi_{1i}\left[b_i v^*_i\left(S^N_i\right) - q_j\left(1 - S^N_j\right)\right] = \bar{\varphi}_{1i}$ is fixed at the solution of the short-run problem and aggregate regional energy or, equivalently, use of GHGs is $E_i = E_{c,i} + E_{A,i}$.

Each region takes the action paths of the other region as fixed and solves problem (36). The current value Lagrangians for the problem of each region can be defined as:

strong time consistency – as the feedback Nash equilibrium (FBNE) concept, but there are significant computational advantages of solving open-loop versus feedback which in our case are important given the complexity of the model. Furthermore, the OLNE and the FBNE solutions deviate in the same direction relative to the cooperative equilibrium and may be close to each other.

$$\mathcal{L}_1 = \mathcal{H}_1 + \kappa_1 \left[\varphi_{01}\left(\bar{L}_1 - L_{A,1}, T_1\right) + \bar{\varphi}_{11} - l_{c,1} - l_{A,1}\right] \tag{44}$$

$$\mathcal{H}_1 = \left[\hat{a}_1 \ln C_1 + \hat{b}_1 \ln\left(\bar{L}_1 - L_{A,1}\right)\right] + \lambda_1 \left[E_1(t) + E_2(t) - dX\right] \tag{45}$$

$$\mathcal{L}_2 = \mathcal{H}_2 + \kappa_2 \left[\varphi_{02}\left(\bar{L}_1 - L_{A,1}, T_1\right) + \bar{\varphi}_{12} - l_{c,2} - l_{A,2}\right] \tag{46}$$

$$\mathcal{H}_2 = \left[\hat{a}_2 \ln C_2 + \hat{b}_2 \ln\left(\bar{L}_2 - L_{A,2}\right)\right] + \lambda_2 \left[E_1(t) + E_2(t) - dX\right] + \xi_2 \left[n_2(t) - mN\right], \tag{47}$$

where $\mathcal{H}_i$ are the regional current value Hamiltonians. The Lagrangian multipliers, κ_i, should be interpreted as the sensitivity of the optimal solution to changes in the constrained constants. The costate variable λ_i has the usual interpretation as the shadow cost of the GHGs accumulation or the regional social cost of carbon (SCC), while the costate variable ξ_2 has the interpretation of the shadow value of innovation in the industrial agricultural sector. A solution of problem (36), if it exists, will characterize the OLNE.

The problem represented by (44)–(47) is the two region integrated model. An increase in the use of agricultural land will have a positive impact on regional welfare because it will increase the consumption aggregate and a negative impact because it will increase the contact rate and reduce Nature's input through the reduction in R_i. In this model the impact of accumulated land-augmenting knowledge in, say, bioengineering, can be understood in the following way.

Remark 1. Consider a steady state of (36) without agricultural land-augmenting innovation $\left(L^*_{A,1}, N^* = 1\right)$ and a steady state with land-augmenting innovation $\left(L^{*A}_{A,1}, N^{*A} > 1\right)$. If $\left(N^{*A} L^{*A}_{A,1} \geq L^*_{A,1}, L^{*A}_{A,1} < L^*_{A,1}\right)$, then at the "with innovation" steady state, Nature R_1 increases in the region which is an ID hot spot. This could reduce Nature's impact on long-run ID intensity. Whether an overall reduction in the contact rate takes place depends on the evolution of fossil fuel use and climate change. Knowledge accumulation will be beneficial in each region if $\max J_i^{NA} > \max J_i^N$, $i = 1, 2$, where $\max J_i^{NA}$ stands for maximized welfare under land-augmenting innovation. It should be noted that the assumption that knowledge is accumulated in the North and diffuses freely to the tropics benefits both regions in terms of ID.

6.1.1 Optimality conditions

Problem (36) as represented by (44)--(47) is an optimal control problem with mixed constraints. The optimality conditions (e.g., Seierstad and Sydsaeter, 1986, Chapter 4), under the assumption of interior solutions for the controls to ease exposition, are discussed below and presented in the Appendix 3.

Labor allocation conditions (82) indicate that the marginal product of labor in all uses equals the shadow value of an additional non-infected labor unit plus any marginal labor costs. Energy use in all uses equates the marginal energy cost plus the regional SCC as shown in (83). The aggregate energy flow from each region is given by (88). For land allocation, (84) indicates that in region 1 – the ID hot spot – the marginal product of land allocated to industrial agriculture, defined in terms of effective land ($NL_{A,1}$), should be equal to marginal land-use costs plus the shadow value of total available land in the region weighted by the impact of increasing the use of agricultural land by a small amount on the contact number, plus the marginal cost in terms of reducing Nature's services. Note that the stock of knowledge is decided by the North through (90)–(92). The impact of land-augmenting knowledge can be further clarified with the help of Fig. 3.

{Insert Fig. 3 here}

Point A corresponds to an agricultural land allocation without any knowledge accumulation ($N = 1$). The line AC defines land-use as

$$L_{A,1}(N) = \frac{L_{A,1}(1)}{N},\ N \in [1, \hat{N}].$$

Suppose that knowledge accumulation increases to $\bar{N}$. Then land-use can be reduced to $L_{A,1}(\bar{N})$ with an equivalent increase of land left to Nature, while the effective land input is the same as $L_{A,1}(1)$. This reduces the contact rate in both regions as indicated by (15) and increases ecosystems' contribution to the composite good.

Finally, the cost of climate change is governed by (86) which describes the evolution of the SCC. It can be seen that this social cost in addition to climate change damages includes the impact of temperature on the contact number weighted by the RTCRE.

6.1.2 Policy implications

Optimality condition (84) suggests that the cost of converting one unit of Nature to industrial agriculture consists of two parts. The first is the loss in ecosystem services $\frac{\hat{b}_1}{\bar{L}_1 - L_{A,1}}$ which is the traditional concept used in cost-benefit analysis of conversion vs preservation and in valuations studies such as contingent valuation. The second represents a type of cost emerging from the epi-econ model which reflects the cost in terms of emerging ID associated with the reduction of the natural world in order to increase industrial agriculture, $\kappa_1 \frac{\partial \varphi_{01}}{\partial(\bar{L}_1 - L_{A,1})}$.

Condition (86) suggests that SCC should include, in addition to the standard concept of damages to the economy – in this case, $\hat{a}_i \omega_i \Lambda_i X$ – the extra cost in terms of emerging IDs, $\kappa_i \frac{\partial \varphi_{0i}(R_1, T_1)}{\partial T_1} \omega_1$, induced by a unit of GHG emissions. This extra cost should be considered in carbon pricing.

6.1.3 The OLNE steady state: knowledge

The dynamics of the knowledge subsystem decouple from the dynamics of the climate subsystem. This is because the structure of the problem – which is logarithmic in (NL) along with linear dynamics for knowledge accumulation – makes the optimal R&D flow depend on the shadow value of knowledge only, as indicated by (90)–(92). Then, the steady state is defined as:

$$N = \frac{\xi_2}{\hat{a}_2 c_{n_2} m} \ , \ \xi_2 = \frac{\hat{a}_2 a_{A,2} \beta_{L,A,2}}{(\rho + m) N} \ \text{ or} \tag{48}$$

$$\xi_2^{\infty} = \left(\frac{\hat{a}_2^2 a_{A,2} \beta_{L,A,2} c_{n_2} m}{(\rho + m)} \right)^{1/2} \ , \ N^{\infty} = \frac{\xi_2^*}{\hat{a}_2 c_{n_2} m}. \tag{49}$$

Proposition 2. *The steady state (ξ_2^*, N^*) for knowledge accumulation exists, it is unique and a saddle point.*

For the proof, see Appendix 3.

The convergence to the steady state using a numerical simulation is shown in Section 6.3.

6.1.4 The OLNE steady state: climate

To study the Hamiltonian system (86)–(88) which determines the OLNE for climate, we need to define the optimal controls as functions of the state-costate variables (T_i, λ_i). In order to provide a clear picture of the structure

and properties of this steady state – given the nonlinearity of the optimality conditions for controls (82)–(85) – we consider a linearization of these conditions around the short-run Nash equilibrium, and we assume a linear representation of the inverse of the contact number for the part that depends on Nature and climate, or:

$$\varphi_{0i}\left(R_1, T_1\right) = \gamma_{0i} + \gamma_{iR_i}\left(\bar{L}_1 - L_{A,1}\right) - \gamma_{iT_1} T_1. \tag{50}$$

Solving the linearized first-order conditions for the controls in terms of the multipliers κ_i for (82) and (84) and the costate variables λ_i for (83); substituting the solutions into the constraints associated with the multipliers κ_i; solving for κ_i and substituting the solutions back into (82) and (84), we obtain the land allocation as a function of temperature in region 1 and accumulated knowledge, while energy use is directly related to the regional SCC through (83). These conditions represent the feedback controls for land-labor allocation, energy use and natural world preservation as functions of climate change, the productivity of the economy, the exogenous land availability and the short-term disease-containment parameter. The evolution of the OLNE potentially towards a steady state can be studied by substituting the feedback controls into (86)–(87).

6.1.5 Open loop Nash equilibrium

Since the knowledge system decouples from the climate system, each region replies optimally to the other region's emissions as indicated by (88), and the reply depends only on the region's shadow cost of GHG $\lambda_i(t)$. The regions are not symmetric, therefore their corresponding shadow costs of GHG are expected to be different, $\lambda_1(t) \neq \lambda_2(t)$, while the state variable $X(t)$ is common for both regions. Therefore the OLNE for the climate subsystem should be analyzed in the context of a three-dimensional Hamiltonian system describing the evolution in time of $(X(t), \lambda_1(t), \lambda_2(t))$.

Proposition 3. *There is a unique OLNE steady state* $\mathbf{x}^\infty = (\lambda_1^\infty, \lambda_2^\infty, X^\infty)$ *for the two-region linearized system with the saddle point property.*[30]

[30] We study the properties of the long-run OLNE in the neighborhood of the short-run "static" Nash equilibrium. This seems to be reasonable if an emerging ID has been controlled and the regions or a social planner, as we shall see later, after recognizing the importance of land-use and climate change in IDs, seeks long-run optimal policies. The

For the proof, see Appendix 3.

The saddle point stability implies that for any initial value of GHGs in the neighborhood of the steady state initial values and paths for the controls $\mathbf{u}_i$ can be chosen such that the paths for the state variables will converge to the steady state OLNE. Foe more details see Appendix 3.

7 The long-run social optimum

To attain the social optimum a social planner maximizes a social welfare function of the form $\log\left(Z_1^{z_1} Z_2^{z_2}\right)$, subject to the relevant constraints. The planner's current value generalized Hamiltonian is:

$$\begin{aligned}\mathcal{H} = \sum_{i=1}^{2} z_i \left[\hat{a}_i \ln C_i + \hat{b}_i \ln\left(\bar{L}_i - L_{A,i}\right)\right] + \\ \lambda\left[E_1(t) + E_2(t) - dX\right] + \xi_2\left[n_2(t) - mN\right] + \\ \kappa_1\left[\varphi_{01}\left(\bar{L}_1 - L_{A,1}, T_1\right) + \bar{\varphi}_{11} - l_{c,1} - l_{A,1}\right] + \\ \kappa_2\left[\varphi_{02}\left(\bar{L}_1 - L_{A,1}, T_1\right) + \bar{\varphi}_{12} - l_{c,2} - l_{A,2}\right], \end{aligned} \tag{51}$$

with optimality conditions, assuming interior solutions for the controls, discussed below and presented in Appendix 3.

7.1 Discussion of the optimality conditions and policy implications

Optimality conditions for labor allocation and energy use, (103) and (104) respectively, have the same structure as the optimality conditions for the noncooperative solution but with an adjustment for the welfare weights (z_1, z_2), while the shadow cost of GHGs in energy use is now the global SCC and not the regional one. The socially optimal land allocation for agriculture in region 1, (105), takes into account, relative to the noncooperative allocation rule, the ID cost induced in region 2 from reducing the natural world in region 1 in order to increase agricultural land in region 1. This is represented by the term $\frac{\kappa_2 \partial \varphi_{02}}{\partial\left(\bar{L}_1 - L_{1A,1}\right)}$. The SCC, which is the solution of (107), contains two additional terms relative to the noncooperative solution. The term $\sum_{i=1,2} z_i \hat{a}_i \omega_i \Lambda_i^2 X$ represents global economic damages from GHGs. The term $\sum_{i=1,2} \kappa_i \frac{\partial \varphi_{0i}(R_1, \Lambda_1 X)}{\partial X}$ is the global ID cost attributed to

behavior of the full nonlinear system from any initial state and the possibility of multiple steady states should be an area of further study.

the SCC since an increase in the GHGs will have a positive effect on the contact number of IDs emerging in region 1 and affecting region 2 as well. Finally, (112) indicates that the shadow value of knowledge accumulation should take into account the impact of knowledge in both regions.

These results suggest that in order to correct the distortions of the noncooperative solution and try to attain the global social optimum, three distortions should be corrected: the land allocation, SCC and knowledge accumulation distortions. Land allocation implies that region 1 which is an ID hot spot should increase its natural world relative to the noncooperative solution. Given that region 1 is expected to be the less developed region, this realization would support a policy of compensation from the developed region 2 to counterbalance losses in the production of the consumption composite. This compensation could be in the form of payments for ecosystem services, REDD+, or other policies which include transfer of resources from the developed to the developing world, as for example is stated in the Paris Accord and subsequent Conferences of the Parties. The GHG distortion should be addressed by an appropriate increase in the SCC. Finally, correcting for the knowledge distortion could imply subsidizing knowledge accumulation in region 2, which would be reflected in the term $\frac{z_1\hat{a}_1 a_{A,1}\beta_{L,A,1}}{N}$.

7.1.1 The socially optimal steady state

The knowledge system is decoupled from the climate system so the steady state can be characterized as in the noncooperative case. The steady state exists, it is unique and it has the saddle point property and indicates a higher level of knowledge at the steady state relative to the noncooperative steady state. This follows directly by comparing (91) to (112).

For the climate steady state, the following proposition can be stated.

Proposition 4. *Assume that* $\left\{(\kappa_1^*(X), \kappa_2^*(X)), \left(\frac{\kappa_1^*(X)}{\partial X}, \frac{\kappa_2^*(X)}{\partial X}\right)\right\}$ *are positive at the socially optimal solution, then a socially optimal steady state exists and has the saddle point property.*

For the proof, see Appendix 3.

Convergence to the steady state is shown in Section 6.4.

A global social optimum without time separation means that the regions act cooperatively at the containment stage and at the climate and land-use

policy stage, or that some World Authority implements policy. The main result is there exist extra benefits that containment policy in region 1 has on region 2, since reducing the infected in region 1 also generates benefits in region 2 because fewer infected are traveling from 1 to 2. This suggest that containment in region 1 should be subsidized. Details are provided in Appendix 4.

7.2 The full solution: linking the short run and the long run

In the analysis of the optimal short-term disease containment in Section 3, R_1 and T_1 were treated as fixed exogenous parameters. The solution of the long-run problem implies that if the regions follow OLNE or social optimization policies, then the fixed R_1 and T_1 in the short run will be determined by the corresponding OLNE or socially optimal paths at each point in time. Thus the short-run optimal containment policy v_i^* will follow a path $v_i^*(t)$ which will be determined by the long-run solution at the time scale of the climate change and will eventually converge to the OLNE or the socially optimal steady state. Assuming that in the short run, containment policies and susceptibles are determined by the Nash equilibrium, since each region follows own health policies, the solution can be interpreted as the fast time SIS system converging to the slow manifold of the climate system. The path of the Nash equilibrium will be the solution, for $i, j = 1, 2, i \neq j$, of

$$S_i(t) = \varphi_{0i}\left(R_1(t), T_1(t)\right) + \varphi_{1i}\left[b_i\left(\frac{\varphi_{1i}b_i}{c_{v_i}}\right)\zeta_i(S_j(t)) - q_j\left(1 - S_j(t)\right)\right], \quad (52)$$

in which the paths for $R_1(t), T_1(t)$ are either the OLNE paths or the socially optimal paths. Thus the full solution can be thought of as pasting two types of solutions: (1) Long-run: OLNE in long-run control variables – Short-run: Nash equilibrium in short-run control variables; or (2) Long-run: Social optimum in long-run control variables – Short-run: Nash equilibrium in short-run control variables. In Section 8.5, we provide potential solution paths for these two solution concepts.

8 Numerical simulations

This paper builds a model that contains three interrelated building blocks. The first embodies the ideas of epidemiologists, biologists and ecologists about IDs and their relationship to climate change and land-use. The second presents nature in the form of land available for agriculture, and climate

represented in a summary way by the evolution of the temperature anomaly. The third is an economic model which includes a traditional economic optimization of an objective that incorporates controls which: (i) in the short run, optimally contain emerging IDs; and (ii) in the long run, by choosing optimal paths for GHG emissions, land-use and R&D that support the bioeconomy, control the emergence and severity of IDs.

This section does not provide a calibration but rather a numerical simulation, using what we consider as plausible values for the parameters shown in the Appendix 5. The main reason is that a full calibration would require, for example, parameter values such as Nature and climate-dependent contact numbers or efficiency of vaccination policies in different regions. These are areas of current research in other scientific fields and their estimation goes beyond the objectives of the current paper. Our simulations, looked at from this viewpoint, provide qualitative results which suggest that the theory developed in this paper deserves further study. Finally we point out that the long-run simulations focus on the SIS model. As explained earlier, once the short-run equilibrium is defined, the procedure to analyze the long-run is the same whether the model is SIR or SIS.[31]

8.1 Nash equilibrium

Fig. 4 depicts the Nash equilibrium for the SIS model discussed in Section 3.1.1. For our parametrization, a Nash equilibrium exists and at the equilibrium solution the susceptibles act as strategic complements, so the containment effect in one region helps the other region.

{Insert Fig 4 here}

Nash equilibrium is at the intersection of lines 1 and 2 with $S_1 = 0.6, S_2 = 0.724$, which is the solution of system (71)–(72). Line 4 is the 45° line and its intersection with line 3 is the fixed point of (72), since $S_2^N : S_2^N = g_1\left(g_2(S_2^N)\right) = 0.724$, while line 5 with the vertical at $S_2 = 1$ defines the $[0,1] \times [0,1]$ space. The parametrization used implies contact numbers $(\sigma_1, \sigma_2) = (1.66, 1.28)$ at the Nash equilibrium solution. Labor allocation and energy use in the short run are functions of the equilibrium

[31] All calculations and figures were produced using Mathematica 13. We are well aware that most of the "extra" digits in the numerical values reported are not significant, but we report them in the way that the software reports numbers.

level of susceptibles $\left(S_1^N, S_2^N\right)$ and all constraints are satisfied. The higher Nash equilibrium value of susceptibles in region 2 relative to 1 is due to the parametrization which assumed that the initial contact number was lower and the effectiveness of containment policy was higher in region 2 than in 1. Different parameterizations in the neighborhood of the central values used in the simulation yield qualitatively similar results without any large shifts.

8.2 OLNE

To provide a tractable model we linearize the first-order conditions for OLNE around the Nash equilibrium and then calibrate the constants of the emission functions (83), so that the steady state accumulation of CO_2 is approximately 3,300 $GtCO_2$ which is the IPCC (2021) prediction for the SSP1-6 scenario to be reached by around 2050. As mentioned earlier, this exercise is not meant to provide "realistic" paths but rather to serve as a vehicle to clarify theoretical concepts. It suggests that the model can provide an adequate description of a complex problem that combines epidemiology, climate science and economics. Fig. 5 presents the OLNE steady state that shows the saddle point structure with a one-dimensional stable manifold in the three-dimensional state-costate space.

{Insert Fig. 5 here}

The stable manifold is MM' and in our parametrization the system's initial state is M'. This means that, given this initial state for the GHGs state variable X, initial values for the costates can be chosen by projecting M' on the (λ_1, λ_2) space such that the controlled system will converge along MM' to the OLNE steady state S. This steady state is $\lambda_1^* = -11.773, \lambda_2^* = -1.51234, X^* = 3.33054$, with associated negative eigenvalue -0.0282. The costates have the usual interpretation of regional SCC and thus take negative values as shadow costs. The SCC in region 1, the South, is higher than in the North because the South contains the ID reservoir and could induce further costs as the temperature rises.

Fig. 6 presents the time paths for the temperature anomaly (line 2) and land-use (line 1) in region 1 along the stable manifold. The temperature paths are derived by combining (93)–(98) and (3) for the numerical solution of the problem. The path for land-use is obtained from optimality condition (84) noting that the multiplier κ_1 in the long-run solution depends on the

temperature anomaly. The paths for region 2 have similar behavior but we present only region 1 because it is the relevant region for the ID.

{Insert Fig. 6 here}

8.3 Knowledge accumulation, effective land-use and the natural world

Using the parametrization in the Appendix, the knowledge steady state is $N^{\infty} = 1.285$. It is shown in Fig. 7 along with the saddle point structure.

{Insert Fig. 7 here}

The stable manifold is MM'. Starting from the initial state $N = 1$, at M' knowledge converges along the stable manifold to $N^{\infty} = 1.285$, following an optimal path $N^*(t)$. This implies that at the OLNE steady state the same agricultural output in the South can be produced using 22.2% less land relative to the case where no knowledge was generated in the North. This will reduce the severity of the epidemic in both the South and North. Since the original Hamiltonian system for knowledge is nonlinear, the linear manifold MM' should be regarded as the tangent to the nonlinear manifold at the steady state S.

From the OLNE equilibrium the optimal path for land-use in agriculture in region 1 without R&D (that is, $N = 1$ for all $t \geq 0$) is linear and declining in the temperature of region 1, since an increase in temperature is costly in terms of ID. Then, along the OLNE time path for temperature, the corresponding time path for land-use is:

$$L_1^*(t) = 0.496899 + 0.00310047e^{-0.0878197t}. \tag{53}$$

If this path is combined with knowledge accumulation, then a new path for effective land is determined as $L_1^{EF}(t) = N^*(t)L_1^*(t)$. Assume that we want to keep effective land-use equal to $L_1^*(t)$ so that the same effective land input is used but with less physical land, which will imply more land available for Nature. In this case a new path is defined as:

$$L_1^N(t) = \frac{L_1^*(t)}{N^*(t)} \text{ with } L_1^N(t) < L_1^*(t), t > 0.$$

The two paths $\left(L_1^N(t), L_1^*(t)\right)$ are shown in Fig. 8. The difference between the two paths corresponds to the increase in the natural world made

possible by knowledge accumulation.

{Insert Fig. 8 here}

The use of $L_1^N(t)$ is expected to increase utility in both regions since it will reduce the ID cost without reducing land input.

8.4 The long-run social optimum

Using the linearization of the first-order conditions and the same parametrization, the socially optimal steady state has saddle point structure and a one-dimensional stable manifold in the two dimensional state-costates space, as shown in Fig. 9. The socially optimal steady state is $\lambda_{SO}^* = -10.669$, $X_{SO}^* = 2.76631$. The stable manifold starts from the initial state M' and converges to the steady state S. The SCC is lower for region 1 than for 2 since all external costs have been internalized into the maximization of social welfare. The convergence to S indicates that at the social optimum the stock of GHGs and regional temperatures are lower than at the OLNE steady state, as expected from the theory. Fig. 10 presents the time paths for temperature and land-use in region 1 along the stable manifold which are derived in a similar way as those in Fig. 6. The temperature path in Fig. 10 is uniformly below the corresponding path under OLNE, shown in Fig. 6.

{Insert Figs. 9 and 10 here}

8.5 Linking the short run with the long run

We solve system (52) for the short-run Nash equilibrium using the values for $(L_1(t), T_1(t))$ corresponding to $t = \{0, 10, 20, 30, 40, 50, 60\}$ at the social optimum with land-augmenting knowledge accumulation, and the OLNE with and without land-augmenting knowledge accumulation, denoted in Figs. 11 and 12 as "SocOpt with R&D", "OLNE with R&D" and "OLNE" respectively.

{Insert Figs. 11 and 12 here}

The three lines represent the movement of the "fast" Nash equilibrium of the SIS subsystem along the "slow" stable manifold of the climate subsystem. The results suggest that land-augmenting technical change helps to

reduce the infectives, or increase the susceptibles, relative to the absence of such technical change, at both the OLNE and the social optimum. As expected, at the social optimum susceptibles are higher relative to the OLNE. After the initial increase in the susceptibles because of the land-saving technical change, there is a continuous decrease because increasing temperatures increase the contact number, but susceptibles are always above the no technical change case. The difference between susceptibles with and without land-augmenting knowledge accumulation shown in Figs. 11 and 12 persists until the climate subsystem reaches the steady-state OLNE or the socially optimal steady state, as shown in Fig. 5 and Fig. 9 respectively. Susceptibles are higher in region 2 than in region 1 because of the particular parametrization. Repeated runs with different parameterizations did not produce any change in the basic qualitative result. Land-augmenting technical change increases the natural world and reduces the contact number of IDs. The result is stronger, the slower the increase in temperature.

9 Ambiguity and Policy Design

9.1 Containment policy in the short run under aversion to ambiguity and model misspecification

A major issue in the design of containment policies is uncertainty. Uncertainty can be associated with certain crucial parameters of the epi-econ model. It can also be associated with the probabilities of increasing the contact number above one, as the R decreases and T increases due to anthropogenic actions, thus resulting in the emergence of an ID. Although the relevant literature suggests that it is plausible to have increased contact numbers as R and T evolve, we know of no clear evidence regarding the probabilities and their structure. Thus, although it would be possible to modify the model so that the emergence probability depends on R, T, we choose to analyze ambiguity and concerns about misspecification regarding the parameters of the model and the evolution of climate change. Following Hansen and Miao (2018), we explore the implications of aversion to ambiguity and concerns regarding possible misspecifications of the integrated model from the regulators' point of view.

9.1.1 Robustness and entropy penalization

Assume that a parameter ν of the integrated model, such as b_i, φ_{0i}, or φ_{1i}, $i = 1, 2$, has a prior density π, with $\nu \in \mathcal{V}$. In the context of Hansen and Miao's (2018) approach to ambiguity and model misspecification aversion, the regulator solves the problem:

$$\max_{u_i(t)} \min_{\pi} \int_{\mathcal{V}} U_i\left(C_i; \nu\right) \pi\left(\nu\right) d\nu + \kappa_i \int_{\mathcal{V}} \left[\log \pi\left(\nu\right) - \log \hat{\pi}\left(\nu\right)\right] \pi\left(\nu\right) d\nu, \quad (54)$$

where $u_i = (l_{c,i}, E_{c,i}, l_{A,i} E_{A,i}, v_i)$. In (54), aversion to ambiguity and model misspecification is modeled by introducing a fictitious adversarial or minimizing agent (MA) that distorts the baseline prior density of an uncertain parameter, in order to impose a cost on the regulator who is the maximizing agent. This cost reflects the impact of aversion to uncertainty and model misspecification. By designing regulation based on (54), the regulator derives a decision rule which incorporates this aversion.

In (54), $\hat{\pi}\left(\nu\right)$ is the baseline density for the parameter ν, and $\kappa > 0$ is a parameter which penalizes deviations from the baseline density $\hat{\pi}\left(\nu\right)$ with $\int_{\mathcal{V}} \left[\log \pi\left(\nu\right) - \log \hat{\pi}\left(\nu\right)\right] \pi\left(\nu\right) d\nu$ being the relative entropy discrepancy from the baseline density. For $\kappa \to \infty$, the regulator is committed to the baseline density, which can be interpreted as the case in which – when the cost of distorting the prior to the MA is infinite – the decision maker uses the baseline. As $\kappa \to 0$, the distortion tends to the worst case prior. In problem (54), the regulator maximizes utility using the controls of the integrated model, while Nature, acting as the MA, distorts the baseline prior density of parameters associated with the controls. The regulator is concerned about the distortion of the prior of the integrated model parameters and follows robust control regulation. The solution of the minimization part of problem (54) is given (see Hansen and Miao 2018) as:

$$\pi^*\left(\nu\right) = \frac{\exp\left[-\frac{1}{\kappa} U_i\left(C_i; \nu\right)\right] \hat{\pi}\left(\nu\right)}{\int_{\mathcal{V}} \exp\left[-\frac{1}{\kappa} U_i\left(C_i; \nu\right)\right] \hat{\pi}\left(\nu\right) d\nu}. \quad (55)$$

Substituting $\pi^*\left(\nu\right)$ into (54), the objective to be maximized becomes

$$J_i = \max_{u_i(t)} \left\{ -\kappa \log \int_{\mathcal{V}} \exp\left[-\frac{1}{\kappa} U_i\left(C_i; \nu\right)\right] \hat{\pi}\left(\nu\right) d\nu \right\}. \quad (56)$$

We set $\theta = 1/\kappa$ and interpret θ as the robustness parameter. When $\theta \to 0$ ($\kappa \to \infty$), the regulator optimizes using the baseline prior; when $\theta \to \infty$ ($\kappa \to 0$), the regulator optimizes by taking into account the worst case prior. Expanding (56) around $\theta = 0$ and using the cumulant generating function,

we obtain the expansion

$$K_i(\theta,\nu) = \mathbb{E}_{\hat{\pi}}\left[U_i(C_i;\nu)\right] - \frac{\theta}{2}\mathrm{Var}_{\hat{\pi}}\left[U_i(C_i;\nu)\right]. \tag{57}$$

Assume for the stochastic parameter that $\nu \in \mathcal{V} = [\underline{\nu}, \bar{\nu}]$ with mean μ_ν and variance σ_ν^2 in the baseline density. Expanding the $K_i(\theta,\nu)$, we obtain:

$$\mathbb{E}_{\hat{\pi}}\left[U_i(C_i;\nu)\right] \approx U_i(C_i;\mu_\nu) + \frac{U_i''(C_i;\mu_\nu)}{2}\sigma_\nu^2 \tag{58}$$

$$\mathrm{Var}_{\hat{\pi}}\left[U_i(C_i;\nu)\right] \approx \left(U_i'(C_i;\mu_\nu)\right)^2\sigma_\nu^2, \tag{59}$$

where the derivatives of the utility function are taken with respect to the stochastic parameter ν. Then the maximization problem for the regulator in region i becomes

$$J_i = \max_{u_i(t)}\left\{U_i(C_i;\mu_\nu) + \frac{U_i''(C_i;\mu_\nu)}{2}\sigma_\nu^2 - \frac{\theta}{2}\left(U_i'(C_i;\mu_\nu)\right)^2\sigma_\nu^2\right\}. \tag{60}$$

If we disregard higher-order terms, the optimization problem described by (60) suggests that the utility of the decision maker is penalized by a term defined by the marginal utility of a small change in the mean of the ambiguous parameter multiplied by the variance of the baseline prior and the robustness parameter θ. When $\theta \to 0$, the decision maker is an expected utility maximizer and uses the baseline prior.

9.1.2 Regulation under aversion to ambiguity

Keeping regional T_1 and R_1 fixed, we study the impact of increasing the robustness parameter θ on the optimal choice of controls by comparative statics. Increasing the robustness parameter θ means that regulation takes into account distorted priors which deviate from the baseline and, at the limit as $\theta \to \infty$, tend to the worst case scenario. Regulation under aversion to ambiguity implies that after disregarding R_1, T_1 which are constants in the short run, then using (56) after replacing κ with $1/\theta$, the objective of the regulator in region $i = 1, 2$ for the noncooperative case becomes

$$J_i = \max_{u_i(t)}\left\{\hat{a}_i \log C_i - \frac{1}{\theta}\ln\left(\mathbb{E}\exp\left[(-\theta)\,\zeta_i\varphi_{1i}b_i v_i\right]\right)\right\}, \tag{61}$$

subject the constraints of problem (26). The first-order conditions for the optimal containment policy v_i imply

$$v_i^* = \frac{1}{\hat{a}_i c_{v_i}}\frac{\mathbb{E}\exp\left[(-\theta)\,\zeta_i(S_i)\varphi_{1i}b_i v_i\right]\zeta_i(S_i)\varphi_{1i}b_i}{\mathbb{E}\exp\left[(-\theta)\,\zeta_i(S_i)\varphi_{1i}b_i v_i\right]} = g(\theta, v_i;\zeta_i). \tag{62}$$

Proposition 5. *Consider the integrated model (26) and assume that the parameter b_i, which reflects the effectiveness of the containment control, is uncertain with a baseline prior $\hat{\pi}(b_i)$. Then the Nash equilibrium under ambiguity can be defined, while an increase in the robustness parameter θ will reduce containment policy in region i.*

For the proof, see Appendix 3.

Since the ambiguous parameter is on the effectiveness of control efforts against the emerging ID (that is, b_i), if the worst case value of b_i is zero, then when it costs zero for the adversarial agent to harm the regulator through the ambiguous parameter b_i, the best reply of the regulator in the zero sum game is to set $v_i^* = 0$. The intuition is that as θ increases, the aversion of the regulator induces consideration of distorted priors regarding the effectiveness or the cost of the containment policy which are worse relative to the baseline. Thus, less control is exercised, since its effectiveness tends to zero in the worst case scenario. Since the setup can be generalized to a vector of controls represented by a linear combination of specific controls determining containment policy (that is, $b_i v_i = \sum_{j=1}^{J} b_{ij} v_{ij}\,, i = 1, 2$), Proposition 5 suggests that high aversion to ambiguity regarding the effectiveness of a specific control will reduce the use of this control and will potentially increase the use of other controls which are less ambiguous.

9.1.3 Strong preferences for robustness and ambiguity-adjusted Nash equilibrium

Optimal containment policies can be obtained by maximizing (116) and using first-order condition (117) from the proof of Proposition 5 in the Appendix for the optimal choice of v. To simplify, assume that the baseline prior for the effectiveness of parameter b_i is a uniform distribution with

$$\begin{aligned} b_i &\in [m_{b_i}, M_{b_i}], 0 \leq m_{b_i} \leq M_{b_i} \\ \hat{\mu}_{b_i} &= \frac{m_{b_i} + M_{b_i}}{2}, \hat{\sigma}_{b_i}^2 = \frac{(M_{b_i} - m_{b_i})^2}{12}. \end{aligned}$$

Using this assumption in (116) and the moment-generating function of the uniform distribution, we obtain

$$\frac{-1}{\theta} \ln \left(\mathbb{E} \exp \left[(-\theta) \varphi_{1i} b_i v_i \right] \right) =$$

$$\frac{-1}{\theta} \log \left(\frac{\exp \left[(-\theta) \varphi_{1i} \zeta_i M_{b_i} v_i \right] - \exp \left[(-\theta) \varphi_{1i} \zeta_i m_{b_i} v_i \right]}{\theta \varphi_{1i} M_{b_i} v_i - \theta \varphi_{1i} m_{b_i} v_i} \right) = h(\theta, v_i)$$

with

$$\lim_{\theta\to\infty} h(\theta, v_i) = \varphi_{1i}\zeta_i m_{b_i} v_i \ , \ \lim_{\theta\to 0} h(\theta, v_i) = \varphi_{1i}\zeta_i \hat{\mu}_{b_i} v_i.$$

Thus when $\theta \to \infty$, the regulator is infinitely robust and uses the worst case scenario, while when $\theta \to 0$, the regulator uses the baseline prior. With b-ambiguity, the optimal control for the worst case is

$$v_i^{a,w} = \left(\frac{\varphi_{1i} m_{b_i}}{c_{v_i}}\right) \zeta_i(S_j) \, . \tag{63}$$

Considering the b-ambiguity case, the best response function at a fixed time t is defined as:

$$S_i \ = \bar{\varphi}_{0i} + \varphi_{1i}\left[b_i\left(\frac{\varphi_{1i} m_{b_i}}{c_{v_i}}\right)\zeta_i(S_j) - q_j\,(1 - S_j)\right] \quad i, j = 1, 2, i \neq j. \tag{64}$$

Since $m_{b_i} < \hat{\mu}_{b_i}$, the worst case prior for the policy effectiveness implies less control relative to the baseline prior at the Nash equilibrium. The impact of increased aversion to ambiguity regarding the effectiveness of containment policies is a shift of the best response functions towards the origin which implies an increase in the Nash equilibrium share of infecteds. This was verified by the numerical simulations in Section 8.1.

Thus ambiguity regarding the effectiveness of containment measures leads, in a Nash equilibrium, to an increase in the share of infecteds. The effectiveness of containment measures could be related to technical characteristics such as weak effectiveness of vaccines but also to social characteristics such as opposition to social distancing or vaccination. Reduced vaccinations and opposition to containment measures in parts of the world during the COVID-19 pandemic could suggest increased ambiguity regarding the vaccinations.

Consider now the case where the regulator of a region expresses aversion to ambiguity regarding $\bar{\varphi}_{0i}$, the part of the contact number that does not depend on short-run policies. Then from (116) the regulator's problem for region i can be written as

$$J_i = \max_{u_i(t)} \left\{ \log C_i - \frac{1}{\theta} \ln\left(\mathbb{E} \exp\left[(-\theta_i \zeta_i \bar{\varphi}_{0i})\right]\right) \right\}.$$

$$\zeta_i = \zeta_i(S_i^N).$$

Assume that the baseline prior for the policy-independent part of the contact number is a uniform distribution with the worst case being $\bar{\varphi}_{0i} = 0$,

and parameters in the following intervals:

$$\begin{aligned} \bar{\varphi}_{0i} &\in [0, M_i] \\ \hat{\mu}_i &= \frac{M_i}{2}, \hat{\sigma}_i^2 = \frac{(M_i)^2}{12}. \end{aligned}$$

Then, using the moment-generating function for the uniform distribution,

$$h_i(\theta) = -\frac{1}{\theta}\log\left(\mathbb{E}\exp\left[(-\theta\bar{\varphi}_{0i})\right]\right) = -\frac{1}{\theta}\log\left(\frac{\exp\left[(-\theta)\,\zeta_i M_i\right]-1}{\theta\zeta_i M_i}\right).$$

If the regulator in region i is infinitely robust, then $\lim_{\theta\to\infty} h(\theta) = 0$. This means that if aversion to ambiguity regarding the effectiveness of the short-run containment measures b_i tends also to infinity and the worst case is associated with $m_{b_i} = 0$, then as verified by our numerical simulations the inverse of the contact number

$$\hat{S}_i = \frac{1}{\sigma_i} = \bar{\varphi}_{0i} + \varphi_{1i}\left[b_i\left(\frac{\varphi_{1i}m_{b_i}}{c_{v_i}}\right)\zeta_i(S_j) - q_j\,(1-S_j)\right] \to 0,$$

which implies that at the limit the whole population will be infected in the Nash equilibrium. This observation leads to the following claim.

Claim: *Assume that the ambiguity of the regulator about the natural contact number which is uniformly distributed on* $[0, M_i]$ *is very high, that is,* $\theta \to \infty$. *Then the regulator optimizes by taking into account the worst case prior and the only route for reducing the contact number is to reduce ambiguity about the effectiveness of the short-run containment policy, i.e., reduce ambiguity on* b. *When this short-run ambiguity cannot be reduced for voluntary-based containment policies, then supplementary policies such as fines for non-compliers might be necessary.*

Consider now the case in which in region 1 the worst cases for $\bar{\varphi}_{01}$ and b_1 imply at the limit that $\hat{S}_1 \to 0$. In this case the optimizing region 2 will not respond to region 1's choices but will unilaterally adopt containment control policies. The optimal containment policy for region 2 will be:

$$v_2^{a,w} = \frac{\varphi_{2j}\hat{\mu}_{b_2}}{c_{v_2}}\zeta_2(S_2).$$

Then the equilibrium susceptibles in region 2 will be the fixed point of

$$S_2 = \frac{1}{\sigma_2} = \bar{\varphi}_{02} + \varphi_{12}\left[b_i\left(\frac{\varphi_{2j}\hat{\mu}_{b_2}}{c_{v_2}}\zeta_2(S_2)\right)\zeta_2(S_2) - q_j\right].$$

The result is confirmed by simulation which suggests zero susceptibles for one region and a slight drop in the susceptibles of the other region relative to the no-ambiguity Nash equilibrium. This result could explain differences in

infection and policy effectiveness across regions observed during the COVID-19 pandemic.

9.1.4 A generalization

To provide a clearer picture of the noncooperative equilibrium between the two regions for more general baseline priors, we use approximations (57)–(60) and consider ambiguity in the effectiveness of the containment policy, b_i, $i = 1, 2$. Applying (57)–(60), we consider the problem:

$$J_i = \max_{u_i(t)} \left\{ \hat{a}_i \log C_i - \frac{\theta}{2} \hat{\sigma}_{b_i}^2 \left(\zeta_i \varphi_{1i} v_i\right)^2 \right\},$$

subject to the constraints of problem (26) where ζ_i is the Lagrangian multiplier of constraint (27). The optimality condition implies

$$v_i^{*a} = \frac{\zeta_i(S_i^N)\varphi_{1i}\hat{\mu}_{b_i}}{c_i + \theta_{b_i}\left(\zeta_i(S_i^N)^2\hat{\sigma}_{b_i}\varphi_{1i}\right)^2}, \tag{65}$$

where $\hat{\mu}_{b_i}, \hat{\sigma}_{b_i}^2$ are the mean and variance of the baseline prior for ambiguous parameters corresponding to the effectiveness of the containment policy. Let the baseline prior be uniform with $b_i \in [m_{b_i}, M_{b_i}]$, $0 \leq m_{b_i} \leq M_{b_i}$, then (65) can be further simplified by setting $\hat{\mu}_{b_i} = \frac{m_{b_i}+M_{b_i}}{2}, \hat{\sigma}_{b_i}^2 = \frac{\left(M_{b_i}-m_{b_i}\right)^2}{12}$.

Along the lines of Proposition 5, differences across regions in concerns regarding the effectiveness of instruments in reducing the contact number differentiate the optimal values for the containment instruments. The region for which ambiguity about the effectiveness of a costly instrument is stronger will use less of this instrument relative to the region in which ambiguity about the effectiveness of the instrument is relatively smaller. This result can differentiate between containment policies based on voluntary behavior only, versus menus of policies. If the introduction of supplementary policies such as fines for non-compliers is characterized by less ambiguity, it will be used along with voluntary containment policies. Thus ambiguity differentials differentiate the optimal intensity of the use of containment policies and introduce policy tradeoffs. Furthermore, in line with the theory, as $\theta \to 0$ the optimal controls are designed on the baseline prior, while if regulation is designed on the basis of the worst case regarding the effectiveness of the control and $\theta \to \infty$, then minimal control is undertaken.

9.2 Model misspecification in the long-run social optimum and robust control

The impact of ambiguity in the short run was examined in Section 9.1. In this section we study the impact of model misspecification which affects the evolution of the average temperature in each region which in turn affects the contact number. Since the impact of climate change on the emergence of IDs is an issue of current investigation, it is natural to associate misspecification concerns with this impact. This argument suggests that the regulator in each region is concerned about possible misspecification in the sense of Hansen et al. (2006) and Hansen and Sargent (2008) in the dynamics of the system.

Misspecification concerns in the dynamics of climate change are introduced by allowing for a family of stochastic perturbations to a Brownian motion characterizing climate dynamics. The perturbations are defined in terms of measurable drift distortions. The misspecification error which expresses the decisions maker's concerns regarding departures from a benchmark model is reflected in an entropic constraint (Hansen et al., 2006; Hansen and Sargent, 2008). Ambiguity and concerns about the possibility that an adversarial agent (Nature) will choose not the benchmark model but another one within an entropy ball, which will harm the decision maker's objective, are reflected in a quadratic penalty term which is added to the regulator's objective. This type of ambiguity about the actual model versus the benchmark model has also been referred to as model uncertainty.

Hansen and Sargent call the decision maker's optimization problem with a quadratic penalty "the multiplier robust control problem". A crucial parameter of the problem is the robustness parameter, which reflects the decision maker's concerns about model uncertainty or aversion to ambiguity. It has been shown that as the robustness parameter which is positive tends to the limiting value of zero, the decision problem is reduced to the standard optimization problem under risk – that is, a problem with no ambiguity aversion. When the robustness parameter increases from zero, then concerns about model uncertainty increase. These concerns can be introduced by allowing additive distortions to the GHG accumulation equation of the form $\sqrt{\epsilon}\sigma_0^T\left(\eta^T + z\right)$, where σ_0 is volatility and ϵ is a small noise parameter, z is i.i.d and η represents distortions. These concerns will be translated into concerns about temperature anomalies through the TCRE multipliers and

finally to concerns about the long-term part of contact number $\varphi_{0i}\left(R_1, T_1\right)$. If we consider a multiplier robust control problem (e.g., Hansen et al., 2006; Hansen and Sargent, 2008), the penalty associated with the distortion relative to the benchmark model can be expressed as $\frac{\left(\eta^T\right)^2}{2\theta_i^T(\epsilon)}$, $j = R, T$,where $\theta_i^T(\epsilon)$ is the robustness parameter.

Campi and James (1996) have shown that if $\theta_i^T(\epsilon) = \theta_{i0}^T\epsilon$, then as $\epsilon \to 0$, the stochastic robust control problem is reduced to a simpler deterministic robust control problem. Assume that GHGs evolution for a social planner or global regulator with misspecification concerns can be written as:

$$\dot{X} = E_1 + E_2 - dX + \sigma_0^T\eta(t). \tag{66}$$

Then the socially optimal management problem with concerns about model misspecification is:

$$J = \max_{\{u_i(t), R_i(t)\}} \min_{\{\eta^T\}} \int_0^\infty \mathrm{e}^{-\rho t} \sum_{i=1,2} \left[\log C_i(t) + \psi_i \log R_i(t) + \frac{\theta_i^T\left(\eta^T\right)^2}{2}\right] dt,$$

subject to (66) and the rest of the constraints. Note that the social planner may have different regional robustness parameters. This could reflect the different impact in regional temperature and contact numbers when there are deviations from the benchmark model. The first-order condition for the choice of the distortion η by the MA is:

$$\eta^T = \frac{-\lambda\sigma_0^T}{\theta_1^T + \theta_2^T}.$$

Then the evolution of the climate subsystem for (λ, X) under model misspecification concerns will be, after modifying (107) and (108),

$$\dot{\lambda} = (\rho + d)\,\lambda + \sum_{i=1,2} z_i\hat{a}_i\omega_i\Lambda_i X - \sum_{i=1,2} \kappa_i \frac{\partial\varphi_{0i}(R_1, \Lambda_1 X)}{\partial X}$$

$$\dot{X} = E_1^* + E_2^* - dX + \sigma_0^T \frac{-\lambda\sigma_0^T}{\theta_1^T + \theta_2^T}.$$

For $\theta_i^T < \infty$ and assuming that the conditions of Proposition 4 are satisfied, there will be convergence to the steady state along the stable manifold, which will be different than the path and the steady state without misspecification concerns. Let the new path be $X(t) + \delta^T(t)$; this would imply new paths for regional temperatures $\Lambda_i\left(X(t) + \delta^T(t)\right)$. Then the impact on the temperature-dependent contact number would be a new contact number $\varphi_{0i}^T\left(\bar{L}_1 - L_{A,1}, \Lambda_i\left(X(t) + \delta^T(t)\right)\right)$. If misspecification concerns lead to more conservative emissions policies, such policies would reduce the temperature-

dependent contact number.

10 Concluding remarks

Using a two-region model we developed an integrated model that provided a synthesis in which the economy, the natural world, land-use, climate change and IDs are represented by distinct modules which are based on existing literature. The objective was the study of short-term ID containment policy and long-term policies which focus on land-use changes and climate change as drivers of the emergence of IDs. We model noncooperation as short-run and long-run Nash equilibria. In the short run we analyze both SIS and SIR models of epidemics since these models can be appropriate for different types of IDs. Although we provide some very preliminary results regarding the comparison of short-run policies for SIS and SIR epidemics, more insights into this issue might be gained from further research. The short-run and long-run Nash equilibrium outcomes are compared with socially optimal policies for the world economy. The joint interaction of short-run and long-run in this type of fast-slow dynamic model is seldom studied, in the environmental management literature.[32]

The insights obtained from this synthesis suggest that noncooperative containment policies in the short run, during which land-use and climate change effects are considered as fixed, generate – under plausible sufficient conditions – a Nash equilibrium outcome in the level of infections. Long-run noncooperative choices in land-use policy can be modeled as an OLNE.

In terms of policy insights, our model suggests, as expected, that in the short run optimal containment effort is differentiated between SIR and SIS diseases. In the long run, comparison of the welfare optimum with OLNE suggests a policy consisting of instruments which include: (i) payments for ecosystem services or REDD+ to the developing world, or other policies which include transfer of resources from the developed to the developing world, as for example is stated in the Paris Accord and subsequent Conferences of the Parties, to compensate for preserving the natural world from conversion to agricultural land; (ii) potential adjustment of the social cost of carbon to allow for the impact of GHG emissions on the severity of emerging

[32]For some notable exceptions see Song et al. (2002), Grimsrud and Huffaker (2006), Crepin (2007).

IDs, and (iii) subsidies to the the producers of land-augmenting innovation to internalize the associated positive externality. Another result emerging from the integrated model is that, in valuation studies related to the preservation of ecosystems versus conversion using stated preference methods, the potential value of the ecosystem in mitigating future IDs should be included in relevant questionnaires.

We have assumed that the two time scales, fast and slow, are exogenously fixed. Both scales could be endogenous where the slow time scale can be speeded up with more resources devoted to that task. However, some time scales of action are fixed by Nature, such as forest restoration. Future research can also study welfare comparisons under OLNE and FBNE, when controls and states can be adjusted either at separate or at the same time scale.

Ambiguity about the effectiveness of containment policies implies that increased concerns about it lead to weaker policies. The presence of strong ambiguity regarding the part of the containment number that depends on land-use and climate change, and which is exogenous in the short run, could necessitate introduction of additional policies, such as fines to supplement containment policies that are implemented on a voluntary basis.

The OLNE was characterized in the long run when the controls were land-use allocation between agriculture and the natural world, and carbon emissions in each region. In this equilibrium an additional positive externality, over and above existence values, emerges for the natural world while the SCC should be increased relative to the case when the emerging IDs are not taken into account. These adjustments result from the link between land-use, climate change and the contact number of the emerging ID and should be considered in cost-benefit analysis. Ambiguity and concerns about model misspecification may lead to further increase in the SCC.

It was also shown that land-augmenting technical change increases the land available to Nature and reduces the infectives relative to the case of no technical change. These results suggest that this type of technical change could be important in controlling IDs, along with the other potential benefits in terms of augmented ecosystem services.

Further elaboration of the model could analyze productivity differences as well as differences in the quality of aggregate land endowments among regions and the associated impacts on regional policies.

In equations (16) and (17) which define the contact number as a function of policy parameters, the underlying assumption is that $X = \phi_{0i}\left(R_1(t), T_1(t)\right)$, and $Y = \phi_{1i}\left[b_i v\left(t\right)\right) - m_i^{as} S_i\left(t\right)) - q_j\left(1 - S_{jt}\right)]$ are perfect substitutes in "producing" non-infected people S. If, however, X, Y are producing S through a constant elasticity of substitution function with elasticity less than infinity, then there might be an upper bound in how much policies can increase S. Our conjecture is that this upper bound depends on Nature's undisturbed viral reserves and putting a bound on climate change. This could be an interesting area of further research. Introduction of accumulation of produced capital into the economic model and human capital for knowledge accumulation is another area of further research.

In summary, this paper aimed to create a formal quantitative multi-time scale, two-region integrated framework where the policies against ID in the short-run interact with long-run land-use policies and human encroachment policies on areas of viral disease sources, as well as with human-induced climate change with uncertainties at both time scales. Detailed references are given to support the necessity of building this kind of "grand unified theory". We have only scratched the surface of this exciting, potentially important and unexplored research area.

Appendix

Appendix 1 Non cooperative solutions in the short-run

The SIS model

The optimality conditions for problem (26), in which infections I_{jt} in region j are taken as given, imply that:

$$v_i^* = \frac{\zeta_i \varphi_{1i} b_i}{\hat{a}_i c_{vi}} \tag{67}$$

$$\frac{\hat{a}_i a_{c,i} \beta_{l,c,i}}{l_{c,i}^*} = \frac{\hat{a}_i a_{A,i} \beta_{l,A,i}}{l_{A,i}^*} = \hat{a}_i w_{l,i} + \zeta_i \tag{68}$$

$$\frac{a_{c,i} \beta_{c,E,i}}{E_{c,i}^*} = \frac{a_{A,i} \beta_{E,A,i}}{E_{A,i}^*} = c_{E,i}, \tag{69}$$

assuming that marginal labor costs and energy costs are the same in each region for each use, and where ζ_i is the Lagrangian multiplier associated with the constraints defined by combining (27)–(29). Containment policy v_i (e.g., lock-downs) is positive as long as its effectiveness is positive and the multiplier is positive when the constraint holds as strict equality with $\hat{S}_i(t) < 1$. Condition (68) indicates that the optimal labor allocation across the two possible land uses implies equalization of marginal products, while (69) indicates that, at the regional optimum, the marginal cost of energy equals regional marginal costs. Combining (27), (28) and (68) and solving for ζ_i, we can obtain the multiplier as a nonlinear function of S_j, or $\zeta_i = \zeta_i(S_j)$,$i, j = 1, 2$, $i \neq j$. The optimal containment policy can be written as:

$$v_i^* = \left(\frac{\varphi_{1i} b_i}{\hat{a}_i c_{v_i}} \right) \zeta_i(S_j) \, . \tag{70}$$

Substituting conditions (70) into (28), we obtain the nonlinear best response (or reaction) function of each region to the susceptibles of the other. A solution for system (31), if it exists, will provide the short-run optimal containment Nash equilibrium. System (31) can be written as

$$S_i = g_i(S_j) \, , \; S_j = g_j(S_i) \tag{71}$$

$$S_i = g_i \left(g_j(S_i) \right) . \tag{72}$$

Since $S_i \in$ [0,1] and the function $g_i \left(g_j(S_i) \right)$ takes values in $[0, 1]$, the Nash equilibrium can be thought of as a fixed point of (72), since S_i^N : $S_i^N = g_i \left(g_j(S_i^N) \right)$.

The SIR model

Dropping t as before, the optimization problem and its Lagrangian is

$$\max_{u_i} \ln Z_i \qquad \text{subject to} \tag{73}$$

$$l_{c,i} + l_{A,i} = f_i(x_i) \tag{74}$$

$$\mathcal{L}_i = \ln Z_i + \zeta_i \left(f_i(x_i) - l_{c,i} - l_{A,i} \right).$$

In a similar way as in the case of the SIS epidemic, the optimality conditions for problem (73), in which infections in region j are taken as given, are (68) and (69) for the labor and energy choices, while for the epidemic containment policy (e.g., vaccination), the optimal choice for v_i which targets I_i^{max} is the solution of

$$F_i\left(v_i, I_j^{max}, \zeta_i\right) = -\hat{a}_i c_{vi} v_i + \zeta_i f_i'(x_i(v_i)) \frac{\partial x_i}{\partial v_i} = 0 \text{ or} \tag{75}$$

$$F_i\left(v_i, \mathcal{Z}_j, \zeta_i\right) = -\hat{a}_i c_{vi} v_i - \zeta_i \phi_{1i} b_i \ln\left(\bar{\phi}_{0i} + \phi_{1i}\left[b_i v_i - q_j\left(1 - \mathcal{Z}_j\right)\right]\right) = 0. \tag{76}$$

The optimal containment policy v_i^* for the SIR epidemic is implicitly defined by (76). If the conditions for the application of the implicit function theorem are satisfied for a given parametrization, then (76) can be solved for v_i^* as a function of the rest of variables.

To characterize the Nash equilibrium solution, consider a linear approximation of the labor supply function at the maximum impact of the SIR epidemic (33) around $v_i = 0$, which is the short-run no containment policy, defined as

$$f_i\left(x_i(v_i)\right) = \left\{\left[\bar{\phi}_{0i} + \phi_{1i} q_j\left(1 - \mathcal{Z}_j\right)\right]\left[1 - \ln\left[\bar{\phi}_{0i} + \phi_{1i} q_j\left(1 - \mathcal{Z}_j\right)\right]\right]\right\} - \ln\left[\bar{\phi}_{0i} + \phi_{1i} q_j\left(1 - \mathcal{Z}_j\right)\right] v_i.$$

Then (76) implies that

$$v_i^* = \frac{-\zeta_i \ln\left[\bar{\phi}_{0i} - \phi_{1i} q_j\left(1 - \mathcal{Z}_j\right)\right]}{\hat{a}_i c_{vi}}.$$

If we follow that same steps as in the SIS case, the best response functions can be defined for $i, j = 1, 2, i \neq j$, as

$$\mathcal{Z}_i = \left[\bar{\phi}_{0i} + \phi_{1i}\left[b_i v_i^*(\mathcal{Z}_j) - q_j\left(1 - \mathcal{Z}_j\right)\right]\right] \times \left[1 - \ln\left[\bar{\phi}_{0i} + \phi_{1i}\left[b_i v_i^*(\mathcal{Z}_j) - q_j\left(1 - \mathcal{Z}_j\right)\right]\right]\right].$$

A solution for this nonlinear system, if it exists, will provide the short-run optimal-containment Nash equilibrium for the SIR epidemic, evaluated

at the maximum level of infectives during the episode of the SIR epidemic.

Appendix 2: Proof of proposition 1

For an SIS epidemic the optimality conditions, after substituting the labor constraint into the objective function, imply:

$$cv + b\phi_1 w = \frac{\alpha b \phi_1}{\phi_0 + \phi_1 bv} \tag{77}$$

$$\text{or } MC_{SIS} = MB_{SIS}, \tag{78}$$

where MC stands for marginal cost of the ID and MB for marginal benefit from containment. For an SIR epidemic, the corresponding condition is:

$$cv + b\phi_1 w = \frac{\alpha b \phi_1}{\phi_0 + \phi_1 bv} \frac{\ln(\phi_0 + \phi_1 bv)}{[-1 + \ln(\phi_0 + \phi_1 bv)]} \tag{79}$$

$$\text{or } MC_{SIR} = MB_{SIS} \frac{\ln(\phi_0 + \phi_1 bv)}{[-1 + \ln(\phi_0 + \phi_1 bv)]} = MB_{SIR}. \tag{80}$$

Note that $\phi_0 + \phi_1 bv = \frac{1}{\sigma}$. If $\sigma < 1$, the emerging ID is blocked. If $\sigma > 1$, the emerging ID needs to be contained.[33] For an SIS epidemic, $\frac{1}{\sigma}$ cannot be greater than one since for such an epidemic the share of susceptibles is $S \leq 1$. Thus for an SIS, define the constraint set:

$$\mathcal{N} = \left\{ v : v \geq 0, v \leq v_c := \frac{1 - \phi_0}{\phi_1 b} \right\}. \tag{81}$$

Since IDs have been occurring over all of human history despite world public health efforts, studying the case $\frac{1}{\sigma} < 1$ seems to be a reasonable approach. Under this assumption $\frac{\ln(\phi_0 + \phi_1 bv)}{[-1 + \ln(\phi_0 + \phi_1 bv)]} < 1$. Then it follows from (80) that $MB_{SIR} < MB_{SIS}$ and since the MC line is the same for both epidemics with a positive slope $v^*_{SIR} < v^*_{SIS}$ in the constraint set , as shown in Fig. 2, by the intersection of the MC line AB with the MB_{SIS} and MB_{SIR} lines. If the marginal cost of containment is very low like CD, the SIS epidemic will be blocked.

[33] It can be shown that if $\phi_0(R,T) = \exp(-\alpha R)(1 - \exp \beta T)$, then $\phi_0 < 1$ for all R, T in the expression $\phi_0(R,T) + \phi_1 bv$. In our analysis we keep a linear specification of $\phi_0(R,T)$ for tractability.

Appendix 3: Optimality conditions

Optimality conditions for Section 6.1.1

$$\frac{\hat{a}_i a_{c,i}\beta_{l,c,i}}{l_{c,i}} = \frac{\hat{a}_i a_{A,i}\beta_{l,A,i}}{l_{A,i}} = \kappa_i + \hat{a}_i w_{l,i} \tag{82}$$

$$\frac{\hat{a}_i a_{c,i}\beta_{c,E,i}}{E_{c,i}} = \frac{\hat{a}_i a_{A,i}\beta_{A,E,i}}{E_{A,i}} = \hat{a}_i c_{E_i} - \lambda_i \tag{83}$$

$$\frac{\hat{a}_1 a_{A,1}\beta_{L,A,1}}{L_{A,1}} = \hat{a}_1 c_{L,1} + \kappa_1 \frac{\partial\varphi_{01}}{\partial\left(\bar{L}_1 - L_{A,1}\right)} + \frac{\hat{b}_1}{\bar{L}_1 - L_{A,1}} \tag{84}$$

$$\frac{\hat{a}_2 a_{A,2}\beta_{L,A,2}}{L_{A,2}} = \hat{a}_2 c_{L,2} + \frac{\hat{b}_2}{\bar{L}_2 - L_{A,2}} \tag{85}$$

$$\dot{\lambda}_i = (\rho + d)\,\lambda_i + \hat{a}_i \omega_i \Lambda_i^2 X + \kappa_i \frac{\partial\varphi_{0i}(R_1, T_1)}{\partial T_1} \tag{86}$$

$$\dot{X} = E_1^* + E_2^* - dX \tag{87}$$

$$E_i^* = \frac{\Gamma_i}{\hat{a}_i c_{E_i} - \lambda_i} \tag{88}$$

$$\Gamma_i = \hat{a}_i \left(a_{c,i}\beta_{c,E,i} + a_{A,i}\beta_{E,A,i}\right) \tag{89}$$

$$n_2^* = \frac{\xi_2}{\hat{a}_2 c_{n_2}} \tag{90}$$

$$\dot{\xi}_2 = (\rho + m)\,\xi_2 - \frac{\hat{a}_2 a_{A,2}\beta_{L,A,2}}{N} \tag{91}$$

$$\dot{N} = n_2^* - mN. \tag{92}$$

Proof of Proposition 2

Conditions (48) imply the isoclines $N = \frac{\xi_2}{\hat{a}_2 c_{n_2} m}$, $N = \frac{\hat{a}_2 a_{H,2}\beta_{L,A,2}}{(\rho+m)\xi_2}$. The first is a ray from the origin with positive slope, while the second is a rectangular hyperbola in the positive quadrant. Both are continuous, therefore they intersect once at the steady state (ξ_2^*, N^*).

In system (90)–(92), let $\hat{A} = \frac{1}{\hat{a}_2 c_{n_2}}$, $\hat{B} = \hat{a}_2 \hat{a}_{A,2}\beta_{L,A,2}$. The linearized Jacobian for the system is

$$J = \begin{pmatrix} (\rho + m) & \frac{\hat{B}}{(N^\infty)^2} \\ \frac{1}{\hat{A}} & -m \end{pmatrix}.$$

Since trace$J = \rho > 0$ and det$J = -m(\rho + m) - \frac{1}{\hat{A}}\frac{\hat{B}}{N^{*2}} < 0$, then the steady state (ξ_2^∞, N^∞) has the saddle point property.

Proof of Proposition 3

The linearized system can be written as:

$$\dot{X} = \theta_0 + \theta_1\lambda_1 + \theta_2\lambda_2 - dX \tag{93}$$

$$(\theta_0, \theta_1, \theta_2) > (0, 0, 0) \tag{94}$$

$$\dot{\lambda_1} = (\rho + d)\,\lambda_1 + \omega_1\Lambda_1 X + \kappa_1^*\gamma_{1T_1}\Lambda_1 \tag{95}$$

$$\kappa_1^* = \psi_{11} + \psi_{12}\Lambda_1 X\ ,\ (\psi_{11}, \psi_{12}) > (0, 0) \tag{96}$$

$$\dot{\lambda_2} = (\rho + d)\,\lambda_2 + \omega_2\Lambda_2 X + \kappa_2^*\gamma_{2T_1}\Lambda_1 \tag{97}$$

$$\kappa_2^* = \psi_{21} + \psi_{22}\Lambda_1 X\ ,\ (\psi_{21}, \psi_{22}) > (0, 0)\,. \tag{98}$$

The Hamiltonian system at the steady state can be written as

$$A\mathbf{x} = \mathbf{b} \tag{99}$$

$$A = \begin{pmatrix} (\rho + d) & 0 & J_{13}^C \\ 0 & (\rho + d) & J_{23}^C \\ \theta_1 & \theta_2 & -d \end{pmatrix}, \mathbf{x} = \begin{pmatrix} \lambda_1 \\ \lambda_2 \\ X \end{pmatrix}, \mathbf{b} = \begin{pmatrix} -\theta_0 \\ \psi_{11}\gamma_{1T_1}\Lambda_1 \\ \psi_{12}\gamma_{1T_1}\Lambda_1 \end{pmatrix}$$

$$J_{13}^C = (\omega_1\Lambda_1 + \psi_{12}\Lambda_1^2\gamma_{1T_1})\,,\ J_{23}^C = (\omega_2\Lambda_2 + \psi_{22}\Lambda_1^2\gamma_{2T_1}).$$

The eigenvalues of A are non-zero and real, two positive and one negative, or

$$\varrho_1 = \rho + d$$
$$\varrho_{2,3} = \frac{1}{2}\left(\rho \pm \sqrt{4(\theta_1 J_{13}^C + \theta_2 J_{23}^C) + (\rho + 2d)^2}\right).$$

The determinant of A is not zero because the product of eigenvalues of A is not zero, therefore the unique steady state can be obtained as a solution of the linear system (99), or

$$\mathbf{x}^\infty = A^{-1}\mathbf{b}.$$

Since there are one negative and two positive eigenvalues, the OLNE steady state has the saddle point property with a one-dimensional stable manifold.

Discerption of the OLNE steady state The OLNE steady state can be used to determine the corresponding OLNE steady states for the controls for labor, land, energy and the natural world. The solutions $(\lambda_1^\infty, \lambda_2^\infty)$ can

be used to determine energy from the linearized version of (83). The solution for $T_i^{\infty} = \Lambda_i X^{\infty}$ can be used to determine (κ_1^*, κ_2^*) and then labor use and agricultural land-use through the linearized versions of (82), (84). Then the natural world can be obtained as $R_i^{\infty} = \bar{L}_i - L_i^{\infty}$.

Proposition 3 suggests that the regional SCC, and therefore any climate policy based on this concept, should include an additional component related to the impact of climate change on the contact number of the emerging ID. This component is reflected in the term $\kappa_i^* \gamma_{2T_1} \Lambda_1$. The positivity of the term κ_i^* is reasonable because it implies that optimal containment policy in the very short run will improve the overall performance of the system, since this term reflects the sensitivity of the optimal solution to a small change in the short-run optimal containment parameter.

The saddle point stability implies that for any initial value of GHGs in the neighborhood of the steady state, the OLNE paths converging to this steady state can be approximated as:

$$X(t) = A_1 c_{11} e^{-\varrho_1 t} + X^{\infty}\,, X(0) = X_0 \tag{100}$$

$$\lambda_1(t) = A_1 c_{21} e^{-\varrho_1 t} + \lambda_1^{\infty} \tag{101}$$

$$\lambda_2(t) = A_1 c_{31} e^{-\varrho_1 t} + \lambda_2^{\infty}, \tag{102}$$

where the parameters (A, c, ϱ) are calculated at the solution using the appropriate eigenvector and the initial value for the GHG stock, with $-\varrho_1$ the negative eigenvalue. Note that the system evolves in three-dimensional state-costate space because the differential game is asymmetric. Substitution of paths (100)–(102) into the corresponding optimality conditions for the controls will determine the OLNE time paths for the controls which will drive the system to the OLNE steady state. Convergence to the steady state in the three-dimensional state-costate space is shown in Section 6.2.

Optimality conditions for Section 7

$$\frac{z_i\hat{a}_i a_{c,i}\beta_{l,c,i}}{l_{c,i}} = \frac{z_i\hat{a}_i a_{A,i}\beta_{l,A,i}}{l_{A,i}} = \kappa_i + z_i\hat{a}_i w_{l,i} \tag{103}$$

$$\frac{z_i\hat{a}_i a_{c,i}\beta_{c,E,i}}{E_{c,i}} = \frac{z_i\hat{a}_i a_{A,i}\beta_{A,E,i}}{E_{A,i}} = z_i\hat{a}_i c_{E_i} - \lambda \tag{104}$$

$$\frac{z_1\hat{a}_1 a_{A,1}\beta_{L,A,1}}{L_{A,1}} = z_i\hat{a}_1 c_{L,1} + \frac{\kappa_1\partial\varphi_{01}}{\partial\left(\bar{L}_1 - L_{A,1}\right)} + \frac{z_1\hat{b}_1}{\left(\bar{L}_1 - L_{1A,1}\right)} + \frac{\kappa_2\partial\varphi_{02}}{\partial\left(\bar{L}_1 - L_{1A,1}\right)} \tag{105}$$

$$\frac{\hat{a}_2 a_{A,2}\beta_{L,A,2}}{L_{A,2}} = \hat{a}_2 c_{L,2} + \frac{\hat{b}_2}{\left(\bar{L}_2 - L_{A,2}\right)} \tag{106}$$

$$\dot{\lambda} = (\rho + d)\,\lambda + \sum_{i=1,2} z_i\hat{a}_i\omega_i\Lambda_i^2 X + \sum_{i=1,2}\kappa_i\frac{\partial\varphi_{0i}(R_1, \Lambda_1 X)}{\partial X} \tag{107}$$

$$\dot{X} = E_1^* + E_2^* - dX \tag{108}$$

$$E_i^* = \frac{\Gamma_i}{z_i\hat{a}_i c_{E_i} - \lambda} \tag{109}$$

$$\Gamma_i = z_i\hat{a}_i\left(a_{c,i}\beta_{c,E,i} + a_{A,i}\beta_{A,E,i}\right) \tag{110}$$

$$n_2^* = \frac{\xi_2}{\hat{a}_2 z_2 c_{n_2}} \tag{111}$$

$$\dot{\xi}_2 = (\rho + m)\,\xi_2 - \sum_{i=1,2}\frac{z_i\hat{a}_i a_{A,i}\beta_{L,A,i}}{N} \tag{112}$$

$$\dot{N} = n_2^* - mN. \tag{113}$$

Proof of Proposition 4

Using the linear version for the converse of the contact number and following the steps in the proof of Proposition 1, we solve (105) and (106) to obtain $(L_{A,1}, L_{A,2})$ as functions of (κ_1, κ_2). Substituting back in the relevant constraints along with the labor allocation condition we obtain $(\kappa_1^*(X), \kappa_2^*(X))$.

The isoclines are then defined as:

$$|\lambda_{\dot{\lambda}=0} = \frac{-\sum_{i=1,2} z_i \hat{a}_i \omega_i \Lambda_i X - \sum_{i=1,2} \kappa_i^*(X) \gamma_{iT_1} \Lambda_1}{(\rho + d)} \tag{114}$$

$$|\lambda_{\dot{X}=0} = \frac{(\Gamma_1 + \Gamma_2) - (\chi_1 + \chi_2) X + \sqrt{-4 [\chi_1 \chi_2 - (\Gamma_1 \chi_2 + \Gamma_1 \chi_2)] + [(\chi_1 + \chi_2) X - (\Gamma_1 + \Gamma_2)]^2}}{2X} \tag{115}$$

where $\chi_i = z_i \hat{a}_i c_{E_i}$. If $\frac{\kappa_i^*(X)}{\partial X} > 0$, then (114) has the regular for these problems negative slope. If there is an intersection with a part of (115) that has a positive slope, then a steady state exists with the saddle point property. This can be shown by using the linearized, at this steady state, Jacobian matrix of the system (107)–(108) which can be written as:

$$J^S = \begin{pmatrix} (\rho + d) & J_{12}^S \\ J_{21}^S & -d \end{pmatrix},$$

where $J_{12}^S = \left(\sum_{i=1,2} z_i \hat{a}_i \omega_i \Lambda_i + \sum_{i=1,2} \frac{\kappa_i^*(X)}{\partial X} \gamma_{iT_1} \Lambda_1 \right) > 0$, $J_{21}^S = \frac{\partial \left(|\lambda_{\dot{X}=0} \right)}{\partial X} > 0$. Then trace$J^S > 0$, det$J^S < 0$ and the steady state has the saddle point property.

Proof of Proposition 5

The objective of the regulator in region $i = 1, 2$ for the noncooperative case becomes

$$J_i = \max_{u_i(t)} \left\{ \hat{a}_i \log C_i - \frac{1}{\theta} \ln \left(\mathbb{E} \exp \left[(-\theta) \zeta_i \varphi_{1i} b_i v_i \right] \right) \right\}, \tag{116}$$

and the first-order conditions for the optimal containment policy v_i imply

$$v_i^* = \frac{1}{c_{v_i}} \frac{\mathbb{E} \exp \left[(-\theta) \zeta_i(S_i) \varphi_{1i} b_i v_i \right] \zeta_i(S_i) \varphi_{1i} b_i}{\mathbb{E} \exp \left[(-\theta) \zeta_i(S_i) \varphi_{1i} b_i v_i \right]} = g(\theta, v_i; \zeta_i). \tag{117}$$

Assume that a Nash equilibrium for a given value of the robustness parameter θ exists. Taking the total derivative of both sides of the first-order conditions for the optimal containment policy v_i (117) with respect to v and θ, we obtain

$$\begin{aligned} c_i dv_i &= g_\theta d\theta + g_{v_{it}} dv_i \Rightarrow (c_i - g_{v_{it}}) \frac{dv_i}{d\theta} = g_\theta \text{ ,with} \\ g_\theta &= \frac{\partial \left[\frac{\mathbb{E} \exp \left[(-\theta) \zeta_i(S_i^N) \varphi_{1i} b_i v_i \right] \varphi_{1i} b_i}{\mathbb{E} \exp \left[(-\theta) \zeta_i(S_i^N) \varphi_{1i} b_i v_i \right]} \right]}{\partial \theta} = -\varphi_{1i} \zeta_i(S_i^N) v_i \hat{\sigma}_{b_i}^2 \\ g_{v_i} &= -\varphi_{1i} \theta \hat{\sigma}_{b_i}^2. \end{aligned}$$

Then it follows that

$$\frac{dv_i}{d\theta} = \frac{-\varphi_{1i} v_i \hat{\sigma}_{b_i}^2}{\left(c_i + \varphi_{1i} \zeta_i(S_i^N) \theta \hat{\sigma}_{b_i}^2 \right)} < 0.$$

Appendix 4: The global social optimum without time separation

To provide more insight into the issue, we consider a global social optimization problem without time separation, which means that the regions act cooperatively at the containment stage, and at the climate and land-use policy stage, or that some World Authority implements policy. We explore all the different externalities associated with the epi-econ model developed in this paper along with possible policy instruments. The generalized Hamiltonian associated with this problem, for $i = 1, 2, i \neq j$, is:

$$\mathcal{H} = \sum_{i=1}^{2} z_i \left[\hat{a}_i \ln C_i + \hat{b}_i \ln\left(\bar{L}_i - L_{A,i}\right)\right] + \lambda \left[E_1(t) + E_2(t) - dX\right] +$$

$$\xi_2 \left[n_2(t) - mN\right] + \sum_{i=1}^{2} \kappa_i \left[\varphi_{0i}\left(\bar{L}_1 - L_{A,1}, T_1\right) + \bar{\varphi}_{1i} - l_{c,i} - l_{A,i}\right] \quad (118)$$

where

$$\bar{\varphi}_{1i} = \varphi_{1i}\left[b_i v_i - q_j(1 - S_j)\right] \quad (119)$$

and (S_1, S_2) are defined as:

$$S_i = \varphi_{1i}\left[b_i v_i - q_j\left(1 - S_j\right)\right] \quad (120)$$

and the control vector includes the containment parameters, that is,

$$\mathbf{u}_i(t) = \left(l_{c,i}(t), l_{A,i}(t), L_{A,i}(t), E_{c,i}(t), E_{A,i}(t), n_2(t), v_1(t), v_2(t)\right).$$

Then the socially optimal containment policy will be

$$v_1^* = \frac{\kappa_1 \varphi_{11} b_1 + \kappa_2 q_1 \varphi_{11} b_1}{z_1 \hat{a}_1 c_{v_1}} \quad (121)$$

$$v_2^* = \frac{\kappa_2 \varphi_{12} b_2 + \kappa_1 q_2 \varphi_{12} b_2}{z_2 \hat{a}_2 c_{v_2}}. \quad (122)$$

The multipliers κ have the same interpretation as the multipliers ζ in Section 3. The term $\kappa_2 q_1 \varphi_{11} b_1$ captures the extra benefits that containment policy in region 1 has on region 2, since reducing the infected in region 1 also generates benefits in region 2 because fewer infected are traveling from 1 to 2 as seen from (120). The interpretation is the same for the term $\kappa_1 q_2 \varphi_{12} b_2$. The rest of the optimality conditions are the same as those corresponding to (51). The policy implication for the result indicated by (121),(122) is

that the World Authority implementing the solution could subsidize for the extra cost associated with benefits $(\kappa_2 q_1 \varphi_{11} b_1, \kappa_1 q_2 \varphi_{12} b_2)$.

Appendix 5: Numerical simulations

1. Consumption composite

$$Z_i(t) = C_i(t)^{\hat{a}_i} R_i(t)^{\hat{b}_i}, \hat{a}_i > 0, \hat{b}_i > 0, \hat{a}_i + \hat{b}_i < 1, i = 1, 2$$

$$C_i = \left[\left(l_{c,i}^{\beta_{l,c,i}} E_{c,i}^{\beta_{c,E,i}}\right)^{\alpha_{c,i}}\right] \times \left[\left(l_{A,i}^{\beta_{l,A,i}} \left(NL_{A,i}\right)^{\beta_{L,A,i}} E_{A,i}^{\beta_{E,A,i}}\right)^{\alpha_{A,i}}\right] \times \exp\left[-\left(\sum_h w_{l,h,i} l_{h,i} + c_{L,i} L_{A,i} + \sum c_{E,h,i} E_{h,i} + \frac{c_{v,i} v_i^2}{2} + \frac{\omega_i T_i^2}{2} + \frac{c_{n,i} n_2^2}{2}\right)\right]$$

Parameter	Description	Value Region 1	Value Region 2
$\hat{a}_i$	Elasticities	0.7	0.8
$\hat{b}_i$	Elasticities	0.25	0.15
$\alpha_{c,i}$	Elasticities	0.7	0.9
$\beta_{l,c,i}$	Elasticities	0.95	0.8
$\beta_{c,E,i}$	Elasticities	0.05	0.2
$\alpha_{A,i}$	Elasticities	0.3	0.1
$\beta_{l,A,i}$	Elasticities	0.6	0.6
$\beta_{L,A,i}$	Elasticities	0.35	0.2
$\beta_{E,A,i}$	Elasticities	0.05	0.2
$c_{h,E,i}$	cost of energy $h = c, A$	$c_{cE} = 0.05, c_{cA} = 0.02$	$c_{cE} = c_{cA} = 0.025$
$w_{l,i}$	cost of labor use	0.3	0.78
$c_{L,i}$	cost of land-use	0.1	0.2
c_{vi}	cost of containment	0.02	0.02
c_{ni}	cost of knowledge	-	0.45
m	knowledge depreciation	-	0.4
$\bar{L}$	regional natural world	1	1
$L_{A,1}$	natural world used*	0.5	0.5

(*) The values are fixed for short-run Nash.

The cost parameters reflect proportional loss in utility from a small increase in the corresponding cost item. Costs are measured in \$/period.

Depreciation rates represent exponential depreciation. The natural world is normalized to 1. By normalizing to 1, we can talk about the fraction of land taken up by agriculture. As pointed out by FAO,[34] global agricultural land area is about five billion hectares, or 38% of the global land surface. About one-third is used as cropland, while the remaining two-thirds consist of meadows and pastures for grazing livestock. Knowledge is measured by investment in R&D expenditures (see Hall et al., 2010). The utility discount rate (or the rate of pure time preference) ρ is set at 0.01.[35]

2. The SIS model

$S_i(t)) \equiv \frac{1}{\sigma_i(t))} = \phi_{0i}(R_1, T_1) + \phi_{1i}[b_i v(t)) - m_i^{as} S_i(t)) - q_j(1 - S_{jt})]$

The contact number σ is the number of adequate contacts of a typical infective during the infectious period. The population is normalized to 1 and S, I represent shares.

Parameter	Description	Value Region 1	Value Region 2
ϕ_1	short-run impact on contact number	1	1
b	effectiveness of containment policy	0.1	0.6
m_i^{as}	infected asymptomatic	0.2	0.1
q	regional flow of infected	$q_2 = 0.001$	$q_1 = 0.005$

$\varphi_{0i}(R_1, T_1) = \gamma_{0i} + \gamma_{iR_i}\left(\bar{L}_1 - L_{A,1}\right) - \gamma_{iT_1} T_1$

Parameter	Description	Value Region 1	Value Region 2
γ_{0i}	exogenous component	0.65	0.75
γ_{iR_1}	natural world impact	0.1	0.05
γ_{iT_1}	climate change impact	0.1	0.05
θ_i	robustness parameter	free	free

The pre-containment σ are $\sigma_1 = 2.22, \sigma_2 = 1.48$ for temperature anomaly $T = 1$ the same for both regions.

3. Climate model

$\dot{X}(t) = E_1(t) + E_2(t) - dX(t)$, $X(0) = X_{preindustrial}$, $T_i = \Lambda_i X$

[34] https://www.fao.org/sustainability/news/detail/en/c/1274219/

[35] If the length of the period corresponding to an epidemic episode increases, the utility discount rate should be increased. Running the simulations with different utility discount rates did not indicate any major qualitative differences in the results. For more details about estimating discount rates, see for example the recent paper by Newell et al. (2022).

Parameter	Description	Value Region 1	Value Region 2
Λ_i	$T_i = \Lambda_i CE$	$\Lambda_1 = 0.4$	$\Lambda_2 = 0.54$
d	GHG depreciation[2]	0.00287	0.00287

With cumulative emissions $CE2400\text{GtCO}_2$ (IPCC, 2021) and $T_1 = 0.96$ for the tropics and 1.031 for the Northern hemisphere. [36]

4. Damage function: climate

$D_i(T_i) = \exp\left(\frac{-\omega_i T_i^2}{2}\right), T(0) = 0$ Preindustrial temperature anomaly

$T_i = \Lambda_i X$

Calibration for 3°C temperature anomaly, GDP loss in region 1 (Tropics-South) 15%, GDP loss in region 2 (North) 2% (Diffenbaugh and Burke, 2019; Brock and Xepapadeas, 2020b).

Parameter	Description	Value Region 1	Value Region 2
$-\omega_i \Lambda_i^2$	damage coefficient	-0.0180577	-0.00338436

[36] See https://www.metoffce.gov.uk/hadobs/hadcrut4/index.htm

References

Albers, H.J., Lee, K.D., Rushlow, J.R., Zambrana-Torrselio, C., 2020. Disease risk from human-environment interactions: environment and development economics for joint conservation-health policy. Environmental and Resource Economics 76 (4), 929–944.

Almada, A.A., Golden, C.D., Osofsky, S.A., Myers, S.S., 2017. A case for Planetary Health/GeoHealth. GeoHealth 1, 75–78.

Ashworth, M., Cherry, T.L., Finnoff, D., Newbold, S.C., Shogren, J.F., Thunström, L., 2022. COVID-19 research and policy analysis: contributions from environmental economists. Review of Environmental Economics and Policy 16 (1), 153–167.

Augeraud-Véron, E., Fabbri, G., Schubert, K., 2021. Prevention and mitigation of epidemics: biodiversity conservation and confinement policies. Journal of Mathematical Economics 93, 102484.

Barbier, E.B., 2021. Habitat loss and the risk of disease outbreak. Journal of Environmental Economics and Management 108, 102451.

Barrows, G., Sexton, S., Zilberman, D., 2014. The impact of agricultural biotechnology on supply and land-use. Environment and Development Economics 19 (6), 676–703.

Berger, L., Berger, N., Bosetti, V., Gilboa, I., Hansen, L.P., Jarvis, C., Marinacci, M., Smith, R.D., 2021. Rational policymaking during a pandemic. PNAS 118.

Biswas, N., Avinash Aslekar, A., 2022. Improving agricultural productivity: use of automation and robotics. 2022 International Conference on Decision Aid Sciences and Applications (DASA).

Bloom, D. E., M. Kuhn, and K. Prettner., 2022. Modern infectious diseases: macroeconomic impacts and policy responses. Journal of Economic Literature 60:85-131

Boppart, T., Harmenberg, K., Hassler, J., Krusell, P., Olsson, J., 2020. Confronting epidemics: the need for epi-econ IAMs. Konjunkturinstitutet. Available at https://www.konj.se/download/18.3891afad1764bc62ba84a0e3/1608119814917/Specialst

Borremans, B., Faust, C., Manlove, K.R., Sokolow, S.H., Lloyd-Smith, J.O., 2019. Cross-species pathogen spillover across ecosystem boundaries: mechanisms and theory. Philosophical Transactions of the Royal Society B 374 (1782), 20180344.

Brock, W., Xepapadeas, A., 2020a. The economy, climate change and

infectious diseases: links and policy implications. Environmental and Resource Economics 76, 811–824.

Brock, W., Xepapadeas, A., 2020b. Regional climate policy under deep uncertainty: robust control and distributional concerns. Environment and Development Economics.

Campi, M.C., James, R.M., 1996. Non-linear discrete time risk-sensitive optimal control. International Journal of Robust and Nonlinear Control 6, 1–19.

Crepin, A-S., 2007. Using fast and slow processes to manage resources with thresholds. Environmental and Resource Economics 36:191-213.

Dangerfield, C., E. P. Fenichel, D. Finnoff, N. Hanley, S. H. Heap, J. F. Shogren, and F. Toxvaerd., 2022. Challenges of integrating economics into epidemiological analysis of and policy responses to emerging infectious diseases. Epidemics 39:100585.

Delamater, P.L., Street, E.J., Leslie, T.F., Yang, Y.T., Jacobsen, K.H., 2019. Complexity of the basic reproduction number (R0). Emerging Infectious Diseases 25 (1), 1.

Diffenbaugh, N.S., Burke, M., 2019. Global warming has increased global economic inequality. PNAS 116, 9808–9813.

Dobson, A., Ricci, C., Boucekkine, R., Gozzi, F., Fabbri, G., Loch-Temzelides, T., Pascual, M., 2023. Balancing economic and epidemiological interventions in the early stages of pathogen emergence. Science Advances 9 (21).

Eichenbaum, M.S., Rebelo, S., Trabandt, M., 2020. The macroeconomics of epidemics. National Bureau of Economic Research [preprint]. Available at http://doi.org/10.3386/ w26882.

ENSIA, 2020. Destruction of habitat and loss of biodiversity are creating the perfect conditions for diseases like covid-19 to emerge. Available at https://ensia.com/features/covid-19-coronavirus-biodiversity-planetary-health-zoonoses/.

Evans, T., Olson, S., Watson, J., Gruetzmacher, K., Pruvot, M., Jupiter, S., Wang, S., Clements, T., Jung, K., 2020. Links between ecological integrity, emerging infectious diseases originating from wildlife, and other aspects of human health – an overview of the literature. The Wildlife Conservation Society. Available at https://oxfordinberlin.eu/files/wcslinksbetweenecologicalintegrityandeids

Faust, C.L., McCallum, H.I., Bloomfield, L.S.P., Gottdenker, N.L., Gille-

spie, T.R., Torney, C.J., Dobson, A.P., Plowright, R.K., 2018. Pathogen spillover during land conversion. Ecology Letters 21 (4), 471–483.

Fenichel, E. P., T. J. Richards, and D. Shanafelt., 2014. The control of invasive species on private property with neighbor-to-neighbor spillovers. Environmental and Resource Economics 59:231-255.

Foley, J.A., DeFries, R., Asner, G.P., Barford, C., Bonan, G., Carpenter, S.R., Chapin, F.S., Coe, M.T., Daily, G.C., Gibbs, H.K., et al., 2005. Global consequences of land-use. Science 309 (5734), 570–574.

Friedlingstein, P. et al. (2023), Global Carbon Budget 2023, Earth Syst. Sci. Data, 15, 5301–5369, https://doi.org/10.5194/essd-15-5301-2023, 2023

Gollier, C., 2020. Cost–benefit analysis of age-specific deconfinement strategies. Journal of Public Economic Theory 22 (6), 1746–1771.

Gomes, E., Inácio, M., Bogdzevič, K., Kalinauskas, M., Karnauskaitė, D. and Pereira, P., 2021. Future land-use changes and its impacts on terrestrial ecosystem services: A review. Science of The Total Environment, 781, p.146716.

Graham, J.P., Leibler, J.H., Price, L.B., Otte, J.M., Pfeiffer, D.U., Tiensin, T., Silbergeld, E.K., 2008. The animal-human interface and infectious disease in industrial food animal production: rethinking biosecurity and biocontainment. Public Health Reports 123 (3), 282–299.

Grimsrud, K. M., and R. Huffaker., 2006. Solving multidimensional bioeconomic problems with singular-perturbation reduction methods: Application to managing pest resistance to pesticidal crops. Journal of Environmental Economics and Management 51:336-353.

Guo, Y., Ryan, U., Feng, Y., Xiao, L., 2022. Association of common zoonotic pathogens with concentrated animal feeding operations. Frontiers in Microbiology, 12, 4225.

Hall, B.H., Mairesse, J., Mohnen, P., 2010. Measuring the returns to R&D. In Handbook of the Economics of Innovation (Vol. 2, pp. 1033-1082). North-Holland.

Hansen, L.P., Miao, J., 2018. Aversion to ambiguity and model misspecification in dynamic stochastic environments. PNAS 115 (37), 9163–9168.

Hansen, L.P., Sargent, T.J., 2008. Robustness. Princeton, NJ: Princeton University Press.

Hansen, L.P., Sargent, T.J., Turmuhambetova, G., Williams, N., 2006. Robust control and model misspecification. Journal of Economic Theory

128 (1), 45–90.

He, Y., Yuan, Q., Mathieu, J., Stadler, L., Senehi, N., Sun, R., Alvarez, P.J., 2020. Antibiotic resistance genes from livestock waste: occurrence, dissemination, and treatment. NPJ Clean Water 3 (1), 4.

Hethcote, H.W., 1989. Three basic epidemiological models. In Levin, S.A., Hallam, T.G., Gross, L.J. (eds), Applied Mathematical Ecology. Berlin, Heidelberg: Springer, pp. 119–144.

Hethcote, H.W., 2000. The mathematics of infectious diseases. SIAM Review 42 (4), 599–653.

Hollenbeck, J.E., 2015. Interaction of the role of Concentrated Animal Feeding Operations (CAFOs) in Emerging Infectious Diseases (EIDS). Infection, Genetics and Evolution 38, 44–46.

Institute of Medicine, 2008. Global climate change and extreme weather events: understanding the contributions to infectious disease emergence. Workshop summary. Washington, DC: The National Academies Press.

IPCC, 2021. Climate Change 2021: The Physical Science Basis. Contribution of Working Group I to the Sixth Assessment Report of the IPCC. Cambridge University Press.

Lancet, 2021. Enhancing global cooperation to end the COVID-19 pandemic. The LANCET COVID-19 Commission. Available at https://covid19commission.org/enhancin global-cooperation.

Leduc, M., Matthews, H.D., de Elia, R., 2016. Regional estimates of the transient climate response to cumulative CO2 emissions. Nature Climate Change 6, 474–478.

Lo Iacono, G., Cunningham, A.A., Fichet-Calvet, E., Garry, R.F., Grant, D.S., Leach, M. et al., 2016. A unified framework for the infection dynamics of zoonotic spillover and spread. PLoS Neglected Tropical Diseases 10 (9), e0004957.

Marani, M., Katul, G.G., Pan, W.K., Parolari, A.J., 2021. Intensity and frequency of extreme novel epidemics. PNAS 118 (35), e2105482118.

Martin, I.W.R., Pindyck, R.S., 2015. Averting catastrophes: the strange economics of Scylla and Charybdis. American Economic Review 105 (10), 2947–2985.

Matthews, H.D., Gillett, N.P., Stott, P.A., Zickfield, K., 2009. The proportionality of global warming to cumulative carbon emissions. Nature 459, 829–833.

Meredith, M., Sommerkorn, M., Cassotta, S., Derksen, C., Ekaykin, A., Hollowed, A., Kofinas, G., Mackintosh, A., Melbourne-Thomas, J., Muelbert, M.M.C., et al., 2019. Polar regions. In IPCC Special Report on the Ocean and Cryosphere in a Changing Climate, chapter 3.

Miralha, L., Muenich, R.L., Schaffer-Smith, D., Myint, S.W., 2021. Spatiotemporal land-use change and environmental degradation surrounding CAFOs in Michigan and North Carolina. Science of The Total Environment, 800, 149391.

Mora, C., McKenzie, T., Gaw, I.M., Dean, J.M., von Hammerstein, H., Knudson, T.A., Setter, R.O., Smith, C.Z., Webster, K.M., Patz, J.A., Franklin, E.C., 2022. Over half of known human pathogenic diseases can be aggravated by climate change. Nature Climate Change 12 (9), 869–875.

Newell, R.G., Pizer, W.A., Prest, B.C., 2022. A discounting rule for the social cost of carbon. Journal of the Association of Environmental and Resource Economists, 9 (5), 1017-1046.

Nova, N., Athni, T.S., Childs, M.L., Mandle, L., Mordecai, E.A., 2022. Global change and emerging infectious diseases. Annual Review of Resource Economics 14, 333–354.

Pike, J., Bogich, T., Elwood, S., Finnoff, D.C. and Daszak, P., 2014. Economic optimization of a global strategy to address the pandemic threat. Proceedings of the National Academy of Sciences, 111(52), pp.18519-18523.

Reeling, Carson J., and Richard D. Horan., 2015. Self-protection, strategic interactions, and the relative endogeneity of disease risks. American Journal of Agricultural Economics 97, no. 2, 452-468.

Roberts, M., Dobson, A., Restif, O., Wells, K., 2021. Challenges in modelling the dynamics of infectious diseases at the wildlife-human interface. Epidemics 37, 100523.

Sachs, J., 2001. Tropical underdevelopment. NBER Working paper 8119, National Bureau of Economic Research.

Seierstad, A., Sydsaeter, K., 1986. Optimal Control Theory with Economic Applications. Elsevier North-Holland, Inc.

Smith, K.F., Goldberg, M., Rosenthal, S., Carlson, L., Chen, J., Chen, C., Ramachandran, S., 2014. Global rise in human infectious disease outbreaks. Journal of the Royal Society Interface 11 (101).

Song, B., C. Castillo-Chavez, and J. P. Aparicio., 2002. Tuberculosis models with fast and slow dynamics: the role of close and casual contacts.

Mathematical Biosciences 180:187-205.

Tagne, G.V., Dowling, C., 2020. Land-use controls on nutrient loads in aquifers draining agricultural and mixed-use karstic watersheds. Environmental Monitoring and Assessment 192 (3), 168.

The Independent Panel for Pandemic Preparedness and Response, 2021. COVID-19: Make it the last pandemic. Available at https://www.unaids.org/en/resources/presscentr panel-pandemic-preparedness-response.

Thunström, L., Newbold, S.C., Finnoff, D., Ashworth, M., Shogren, J.F., 2020. The benefits and costs of using social distancing to flatten the curve for COVID-19. Journal of Benefit-Cost Analysis 11 (2), 179–195.

Walsh, M.G., De Smalen, A.W., Mor, S.M., 2018. Climatic influence on anthrax suitability in warming northern latitudes. Scientific Reports 8 (1).

Watts, N., Amann, M., Arnell, N. et al., 2021. The 2020 report of the Lancet Countdown on health and climate change: responding to converging crises. Lancet 397, 129–170.

White, R.J., Razgour, O., 2020. Emerging zoonotic diseases originating in mammals: a systematic review of effects of anthropogenic land-use change. Mammal Review 50 (4), 336–352.

Winkler, K., Fuchs, R., Rounsevell, M. et al., 2021. Global land-use changes are four times greater than previously estimated. Nature Communication 12, 2501 . https://doi.org/10.1038/s41467-021-22702-2

Wyns, A. 2020. Climate change and infectious diseases. Scientific American. Available at https://blogs.scientificamerican.com/observations/climate-change-and-infectious-diseases/.

Xepapadeas, A., 1995. Induced technical change and international agreements under greenhouse warming. Resource and Energy Economics, 17(1), pp.1-23.

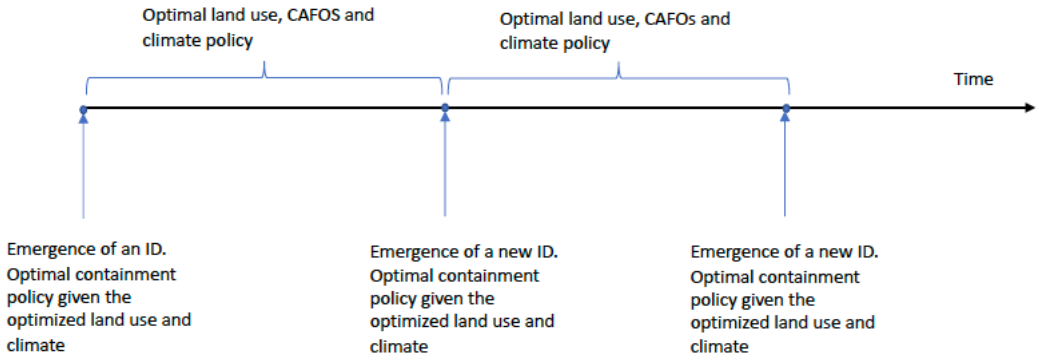

Fig. 1. Emergence of IDs and the timing of policies.

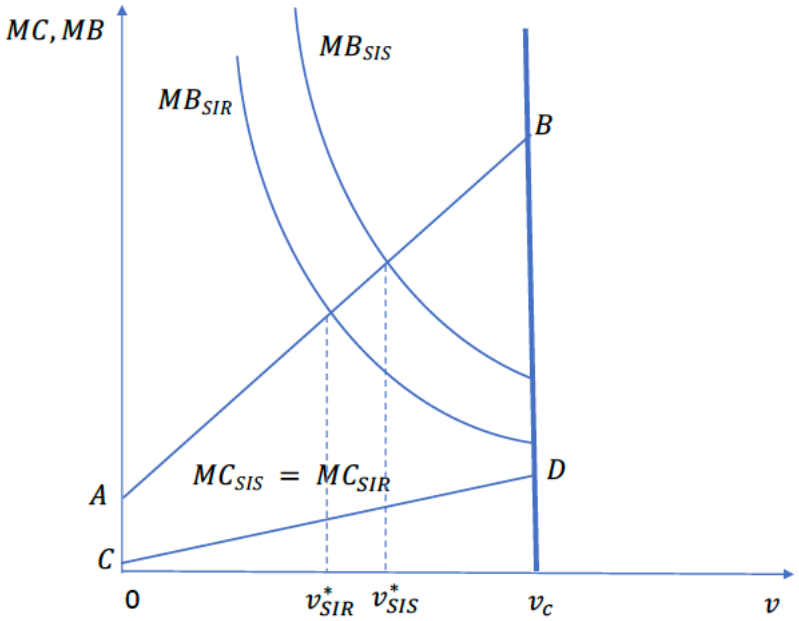

Fig. 2. Short-run containment for SIS and SIR epidemics.

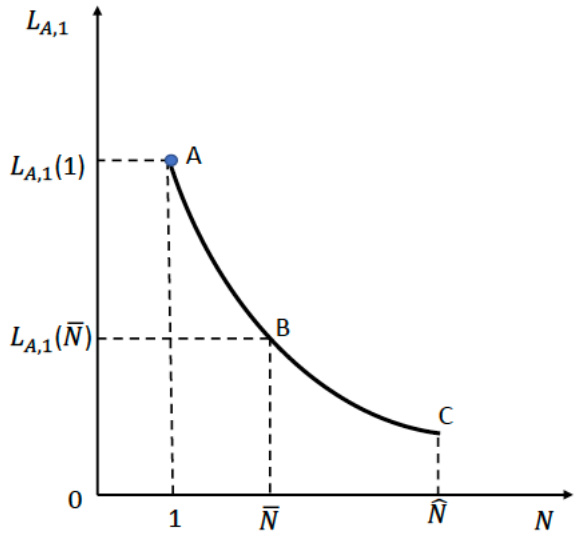

Fig. 3. The impact of land-augmenting technology.

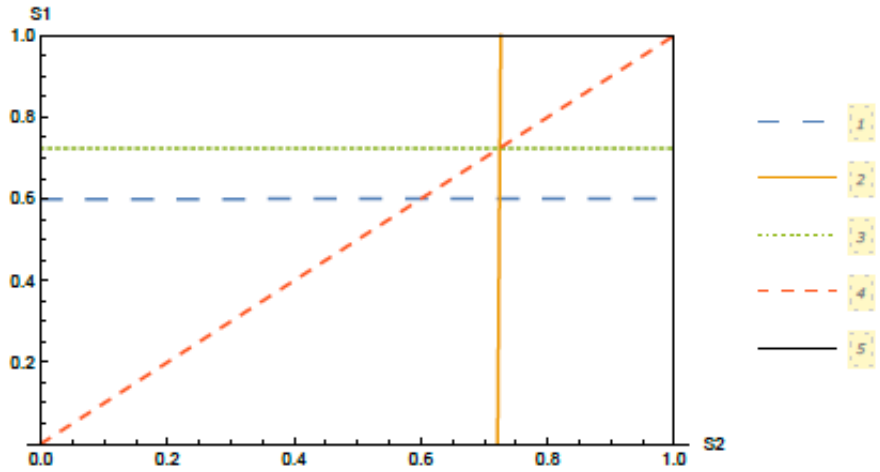

Fig. 4. Nash equilibrium.

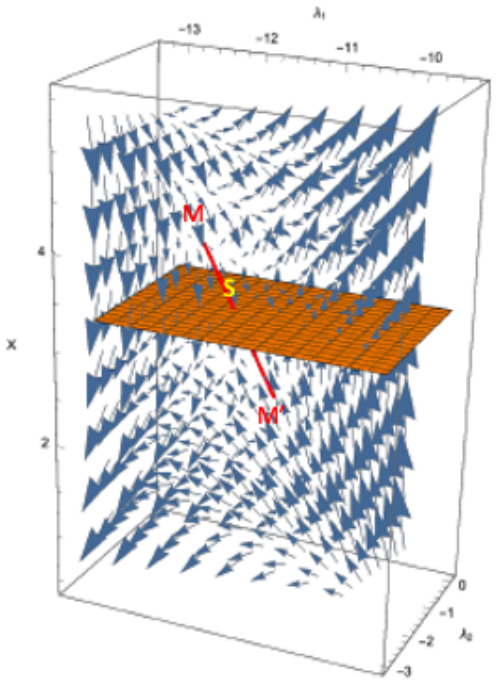

Fig. 5. The OLNE in the three-dimensional state-costate space. The OLNE is derived from system (93)–(98) as shown in the proof of Proposition 3 (Appendix).

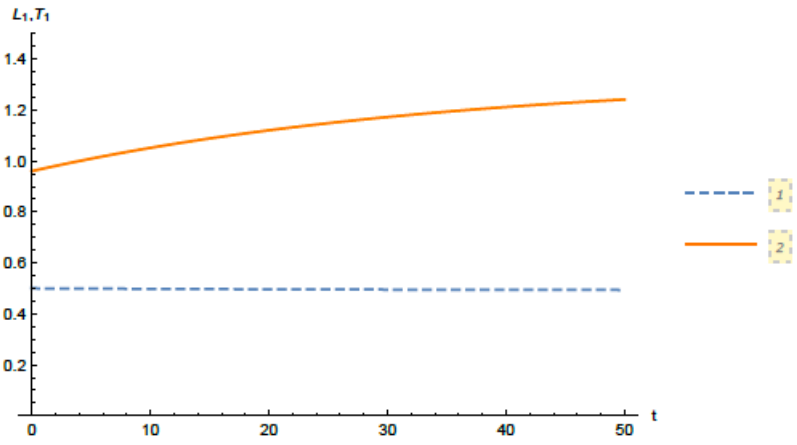

Fig. 6. Time paths for temperature and land-use in region 1 at the OLNE.

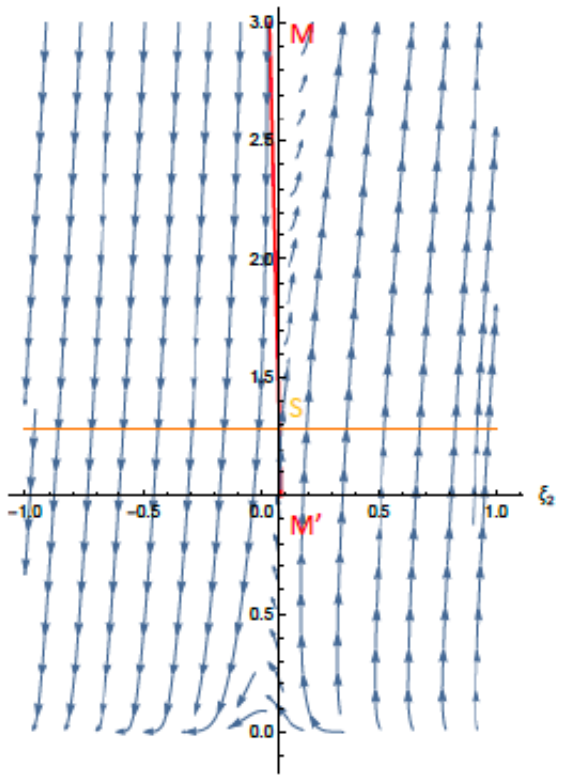

Fig. 7. The saddle point steady state for knowledge. The steady state is derived from Eqs. (90)–(92) as shown in the proof of Proposition 2 (Appendix).

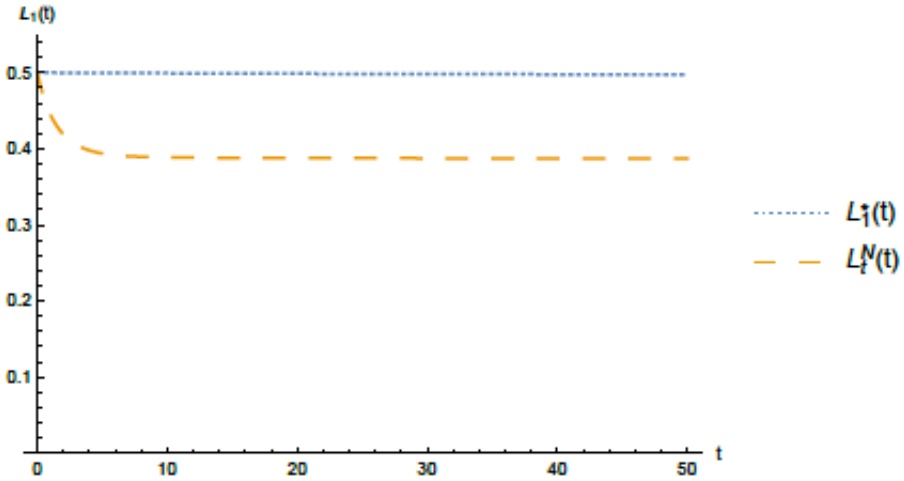

Fig. 8. Gains in the natural world due to R&D.

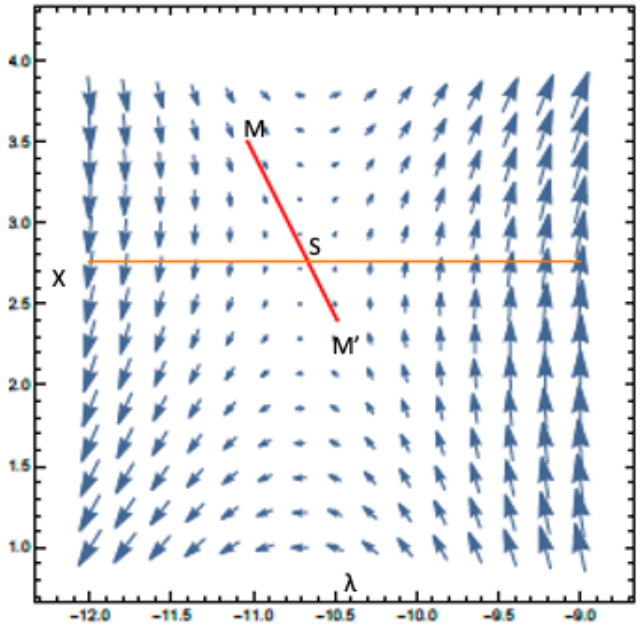

Fig. 9. The socially optimal steady state, derived from (107)–(108).

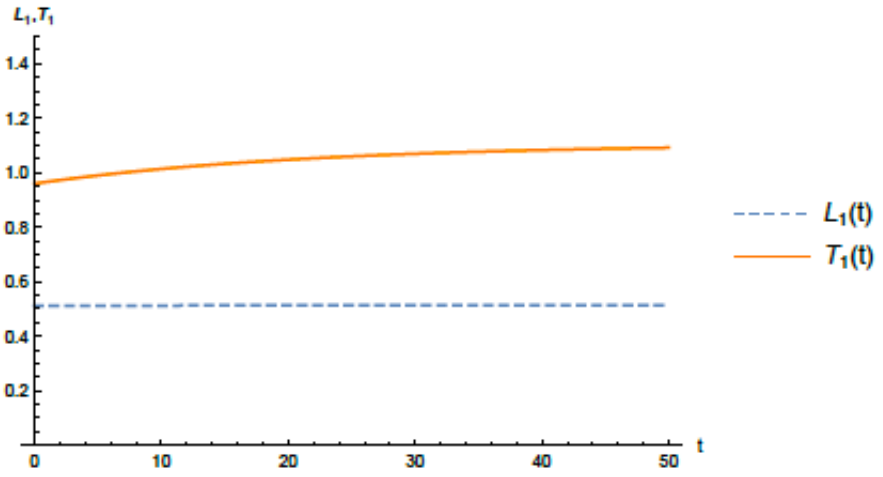

Fig. 10. Time paths for temperature and land-use in region 1 at the social optimum.

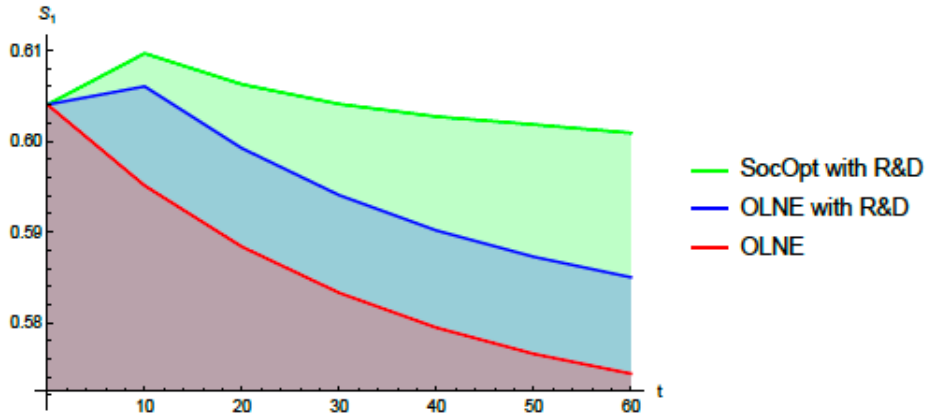

Fig. 11. Susceptibles paths in region 1 with and without land-augmenting knowledge accumulation.

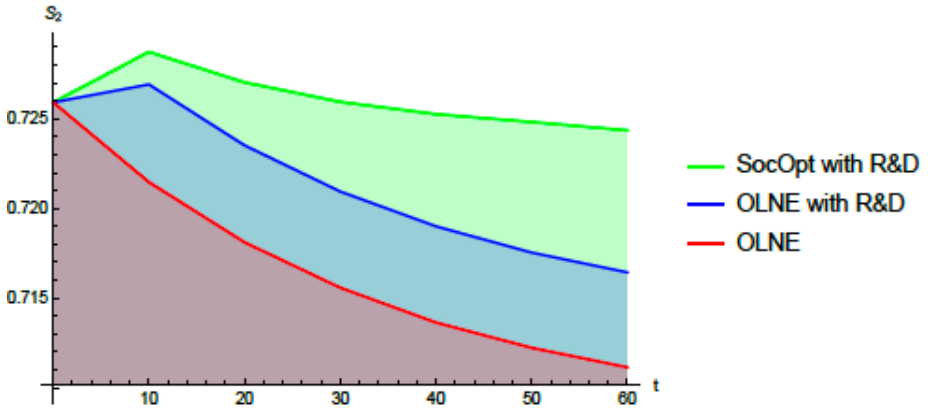

Fig. 12. Susceptibles paths in region 2 with and without land-augmenting knowledge accumulation.